Inorg. Chem. **2007**, *46*, 6811–6826

Square-Planar Rhodium(I) Complexes Partnered with [*arachno*-6-SB_9H_{12}]$^-$: A Route toward the Synthesis of New Rhodathiaboranes and Organometallic/Thiaborane Salts

Álvaro Álvarez, Ramón Macías,* María José Fabra, Maria L. Martín, Fernando J. Lahoz, and Luis A. Oro

Departamento de Química Inorgánica, Instituto Universitario de Catálisis Homogénea, Instituto de Ciencia de Materiales de Aragón, Universidad de Zaragoza-Consejo Superior de Investigaciones Científicas, 50009-Zaragoza, Spain

Received April 4, 2007

Treatment of [RhCl(η^4-diene)]$_2$ (diene = nbd, cod) with the N-heterocyclic ligands 2,2′-bipyridine (bpy), 4,4′-dimethyl-2,2′-bipyridine (Me_2bpy), 1,10-phenanthroline (phen), and pyridine (py) followed by addition of Cs[*arachno*-6-SB_9H_{12}] affords the corresponding salts, [Rh(η^4-diene)(L_2)][SB_9H_{12}] [diene = cod, L_2 = bpy (**1**), Me_2bpy (**3**), phen (**5**), $(py)_2$ (**7**); diene = nbd, L_2 = bpy (**2**), Me_2bpy (**4**), phen (**6**), $(py)_2$ (**8**)]. These compounds are characterized by NMR spectroscopy and mass spectrometry, and in addition, the cod–Rh species **1** and **3** are studied by X-ray diffraction analysis. These saltlike reagents are stable in the solid state, but in solution the rhodium(I) cations, [Rh(η^4-diene)(L_2)]$^+$, react with the polyhedral anion [SB_9H_{12}]$^-$ leading to a chemistry that is controlled by the d^8 transition element chelates. The nbd–Rh(I) complexes react faster than the cod–Rh(I) counterparts, leading, depending on the conditions, to the synthesis of new rhodathiaboranes of general formulas [8,8-(L_2)-*nido*-8,7-$RhSB_9H_{10}$] [L_2 = bpy (**9**), Me_2bpy (**10**), phen (**11**), $(py)_2$ (**12**)] and [8,8-(L_2)-8-(L′)-*nido*-8,7-$RhSB_9H_{10}$] [L′ = PPh_3, L_2 = bpy (**13**), Me_2bpy (**14**), phen (**15**); L′ = $NCCH_3$, L_2 = bpy (**16**), Me_2bpy (**17**), phen (**18**)]. Compound **13** is characterized by X-ray diffraction analysis confirming the 11-vertex *nido*-structure of the rhodathiaborane analogues **14**–**18**. In dichloromethane, **1** and **3** yield mixtures that contain the 11-vertex rhodathiaboranes **9** and **10** together with new species. In contrast, the cod–Rh(I) reagent **5** affords a single compound, which is proposed to be an organometallic rhodium complex bound *exo*-polyhedrally to the thiaborane cage. In the presence of H_2(g) and stoichiometric amounts of PPh_3, the cod–Rh(I) reagents, **1**, **3**, and **5**, afford the salts [Rh($H)_2$(L_2)($PPh_3)_2$][SB_9H_{12}] [L_2 = bpy (**19**), Me_2bpy (**20**), phen (**21**)]. Similarly, in an atmosphere of CO(g) and in the presence of PPh_3, compounds **1**–**6** afford [Rh(L_2)($PPh_3)_2$(CO)][SB_9H_{12}] (L_2 = bpy (**22**), Me_2bpy (**23**), phen (**24**)]. The structures of **19** and **24** are studied by X-ray diffraction analysis. The five-coordinate complexes [Rh(L_2)($PPh_3)_2$(CO)]$^+$ undergo PPh_3 exchange in a process that is characterized as dissociative. The observed differences in the reactivity of the nbd–Rh(I) salts versus the cod–Rh(I) analogues are rationalized on the basis of the higher kinetic lability of the nbd ligand and its faster hydrogenation relative to the cod diene.

Introduction

The chemistry of metallacarboranes has been reasonably well-studied, and it remains an active research area.[1] In contrast, the reactivity of metallaboranes has been less developed, albeit the published results are important.[2] Thus, the general route to metallaboranes through the reactions of boranes with transition-element complexes, and the more specific method through the treatment of monocyclopentadienyl metal halides of groups 5−9 with monoboranes, have permitted the systematic study of their chemistry.[3] These studies have resulted in new metallaboranes that challenge well-established electron counting rules[4] and examples of a rich chemistry with small multiply bonded organic molecules. Reductions,[5] stoichiometric and catalytic oligomerizations,[6] complete or partial insertion of heteroatoms (i.e., C or N) into the clusters,[7] and hydrometalations[8] are some of the observed reactions.

* To whom correspondence should be addressed. E-mail: rmacias@unizar.es.

10.1021/ic700648z CCC: $37.00
Published on Web 07/11/2007

In comparison, the reaction chemistry of metallaheteroboranes containing p-block elements in the framework other than carbon is relatively unexplored.[9] This can be attributed in part to the lack of convenient high-yield methods to this subclass of polyhedral boron-containing compounds. Thus, the 11-vertex *nido*-rhodathiaborane [8,8-$(PPh_3)_2$-8,7-$RhSB_9H_{10}$], easily prepared from $[RhCl(PPh_3)_3]$ and [6-*arachno*-$SB_9H_{12}]^-$,[10] is one of the few metallaheteroboranes for which a systematic chemistry has been developed. The study of this PPh_3-ligated rhodathiaborane has demonstrated that the cluster can add a Lewis base without change of the *nido* structure and, additionally, that it can undergo facile substitution of the PPh_3 ligands and *nido* to *closo* transformation, as well as exhibiting other interesting reactivity.[11]

Our interest in thiaborane and transition metal chemistry led us to exploit other synthetic routes toward rhodathiaboranes bearing different rhodium moieties that could permit the development of a comparative chemistry in a series of isoelectronic 11-vertex clusters. We report here the synthesis of new salts of general formulation [Rh(η^4-diene)(L_2)]-$[SB_9H_{12}]$ [diene = cod, nbd; L_2= bpy, Me_2bpy, phen, $(py)_2$], which have been found to be appropriate starting materials for the synthesis of 11-vertex *nido*-rhodathiaboranes that contain either {Rh(L_2)}- or {Rh(L_2)L′}-moieties as cluster constituents [L_2 = bpy, Me_2bpy, phen, $(py)_2$; L′ = PPh_3, $NCCH_3$]. Additionally, these saltlike reagents have permitted a systematic study of the reactivity of square-planar 16-electron complexes [Rh(η^4-diene)(L_2)]$^+$ with the 10-vertex *arachno*-thiaborane [6-$SB_9H_{12}]^-$.

Experimental Section

General Considerations. All reactions were carried out under an argon atmosphere using standard Schlenk-line techniques.[12] Solvents were distilled immediately before use under an argon atmosphere: sodium benzophenone ketyl for hexanes; calcium hydride for dichloromethane. All commercial reagents were used as received without further purification. The 10-vertex *arachno*-thiaborane salt $CsSB_9H_{12}$ was purchased from Katchem. The starting complexes $[RhCl(cod)]_2$ and $[RhCl(nbd)]_2$ were prepared by published methods.[13] Infrared spectra were recorded in KBr with a Perkin-Elmer Spectrum One spectrometer. C, H, and N analyses were carried out in a Perkin-Elmer 2400 CHNS/O analyzer. NMR spectra were recorded on Bruker Avance 300-MHz and AV 400-MHz spectrometers, using ^{11}B, ^{11}B{^{1}H}, ^{1}H, ^{1}H{^{11}B}, ^{1}H{^{11}B-(selective)}, ^{13}C{^{1}H}, and [^{1}H−^{1}H]-COSY techniques. ^{1}H and ^{13}C NMR chemical shifts were measured relative to partially deuterated solvent peaks but are reported in ppm relative to tetramethylsilane. ^{11}B chemical shifts were measured relative to $[BF_3(OEt)_2)]$. ^{31}P (121.48 MHz) chemical shifts were measured relative to H_3PO_4 (85%). The temperature of the probe was calibrated using the temperature dependence of the chemical shifts of methanol. Line-shape analysis of the ^{31}P-spectra of compound **24** at different temperatures was performed with the gNMR program. Errors in activation parameters obtained from the Eyring regression of the rate constants assumed 1 K error in the temperature and 5% error in the constant and were computed by published methods.[14] Mass spectrometry data were recorded on a VG Autospec double-focusing mass spectrometer, on a microflex MALDI-TOF, and on a ESQUIRE 3000+ API-TRAP, operating in either positive or negative modes.

Crystal Structure Determination of 1, 3, 13, 19, and 24. Crystals suitable for X-ray diffraction analysis were obtained by slow diffusion of hexane at 233 K into CH_2Cl_2 solutions of **1**, **3**, **13**, and **24** and by diffusion of diethyl ether into an acetone solution of **4**. X-ray data were collected for all complexes at low temperature [100(2) K for **1**, **3**, **19**, and **24** or 173(2) K for **13**] on a Bruker SMART APEX CCD diffractometer with graphite-monochromated Mo Kα radiation (λ = 0.710 73 Å). Data were corrected for absorption using a multiscan method applied with SADABS program.[15] The structures were solved by direct methods with

(1) (a) Deng, L.; Xie, Z. *Organometallics* **2007**, *26*, 1832−1845. (b) Wang, X.; Jin, G. X. *Chem.—Eur. J.* **2005**, *11*, 5758−5764. (c) Wang, J.-Q.; Ren, C.-X.; Jin, G.-X. *Chem. Commun.* **2005**, 4738−4740. (d) Wang, J.-Q.; Ren, C. X.; Weng, L. H.; Jin, G. X. *Chem. Commun.* **2006**, 162−164. (e) Wang, J. Q.; Herberhold, M.; Jin, G. X. *Organometallics* **2006**, *25*, 3508−3514. (f) Hosmane, N. S.; Maguire, J. A. In *Comprehensive Organometallic Chemistry*; Crabtree, R. H., Mingos, D. M. P., Eds.; Elsevier: Oxford, U.K., 2007; Vol. 3, Chapter 3.05. (g) Franken, A.; Lei, P.; McGrath, T. D.; Stone, F. G. A. *Chem. Commun.* **2006**, 3423−3425. (h) Douglas, T. M.; Molinos, E.; Brayshaw, S. K.; Weller, A. S. *Organometallics* **2007**, *26*, 463−465. (i) Deng, L.; Chan, H. S.; Xie, Z. *J. Am. Chem. Soc.* **2005**, *127*, 13774−13775. (j) Crossley, E. L.; Caiazza, D.; Rendina, L. M. *Dalton Trans.* **2005**, 2825−2826. (k) Clarke, A. J.; Ingleson, M. J.; Kociok-Kohn, G.; Mahon, M. F.; Patmore, N. J.; Rourke, J. P.; Ruggiero, G. D.; Weller, A. S. *J. Am. Chem. Soc.* **2004**, *126*, 1503−1517.

(2) Weller, A. S. In *Comprehensive Organometallic Chemistry*; Crabtree, R. H., Mingos, D. M. P., Eds.; Elsevier: Oxford, U.K., 2007; Vol. 3, Chapter 3.04.

(3) (a) Bould, J.; Bown, M.; Coldicott, R. J.; Ditzel, E. J.; Greenwood, N. N.; Macpherson, I.; MacKinnon, P.; Thornton-Pett, M.; Kennedy, J. D. *J. Organomet. Chem.* **2005**, *690*, 2701−2720. (b) Fehlner, T. P. *Organometallics* **2000**, *19*, 2643−2651. (c) Fehlner, T. P. *Pure Appl. Chem.* **2006**, *78*, 1323−1331.

(4) Le Guennic, B.; Jiao, H.; Kahlal, S.; Saillard, J. Y.; Halet, J. F.; Ghosh, S.; Shang, M.; Beatty, A. M.; Rheingold, A. L.; Fehlner, T. P. *J. Am. Chem. Soc.* **2004**, *126*, 3203−3217.

(5) (a) Ditzel, E. J.; Fontaine, X. L. R.; Greenwood, N. N.; Kennedy, J. D.; Zhu, S. S.; Thornton-Pett, M. *J. Chem. Soc., Chem. Commun.* **1989**, 1762−1763. (b) Bould, J.; Rath, N. P.; Barton, L.; Kennedy, J. D. *Organometallics* **1998**, *17*, 902−907.

(6) (a) Yan, H.; Beatty, A. M.; Fehlner, T. P. *Organometallics* **2002**, *21*, 5029−5037. (b) Yan, H.; Beatty, A. M.; Fehlner, T. P. *Angew. Chem., Int. Ed.* **2001**, *40*, 4498−4501. (c) Shea, S. L.; Jelinek, T.; Perera, S. D.; Stibr, B.; Thornton-Pett, M.; Kennedy, J. D. *Dalton Trans.* **2004**, 1521−1523.

(7) Ditzel, E. J.; Fontaine, X. L. R.; Greenwood, N. N.; Kennedy, J. D.; Sisan, Z.; Stibr, B.; Thorntonpett, M. *J. Chem. Soc., Chem. Commun.* **1990**, 1741−1743.

(8) (a) Yan, H.; Noll, B. C.; Fehlner, T. P. *J. Am. Chem. Soc.* **2005**, *127*, 4831−4844. (b) Yan, H.; Beatty, A. M.; Fehlner, T. P. *J. Am. Chem. Soc.* **2003**, *125*, 16367−16382.

(9) Wesemann, L. In *Comprehensive Organometallic Chemistry*; Crabtree, R. H., Mingos, D. M. P., Eds.; Elsevier: Oxford, U.K., 2007; Vol. 3, Chapter 3.03.

(10) Ferguson, G.; Jennings, M. C.; Lough, A. J.; Coughlan, S.; Spalding, T. R.; Kennedy, J. D.; Fontaine, X. L. R.; Stibr, B. *J. Chem. Soc., Chem. Commun.* **1990**, 891−894.

(11) (a) Volkov, O.; Macías, R.; Rath, N. P.; Barton, L. *Appl. Organomet. Chem.* **2003**, *17*, 409−420. (b) Volkov, O.; Macías, R.; Rath, N. P.; Barton, L. *Inorg. Chem.* **2002**, *41*, 5837−5843. (c) Volkov, O.; Macías, R.; Rath, N. P.; Barton, L. *J. Organomet. Chem.* **2002**, *657*, 40−47. (d) Macías, R.; Rath, N. P.; Barton, L. *Organometallics* **1999**, *18*, 3637−3648. (e) Macías, R.; Rath, N. P.; Barton, L. *Angew. Chem., Int. Ed.* **1999**, *38*, 162−164. (f) Volkov, O.; Rath, N. P.; Barton, L. *Organometallics* **2002**, *21*, 5505−5514.

(12) Shriver, D. F., Drezdzon, M. A. *The Manipulation of Air-Sensitive Compounds*; Wiley-Interscience: New York, 1986.

(13) (a) Abel, E. W.; Bennett, M. A.; Wilkinson, G. *J. Chem. Soc.* **1959**, 3178. (b) Giordano, G.; Crabtree, R. H. *Inorg. Synth.* **1979**, *19*, 218.

(14) Morse, P. M.; Spencer, M. D.; Wilson, S. R.; Girolami, G. S. *Organometallics* **1994**, *13*, 1646.

(15) (a) *SAINT+ Software for CCD diffractometers*; Bruker AXS: Madison, WI, 2000. (b) Sheldrick, G. M. *SADABS Program for Correction of Area Detector Data*; University of Göttingen: Göttingen, Germany, 1999.

SHELXS-86.[16] Refinement, by full-matrix least squares on F^2 with SHELXL97,[16] was similar for all complexes, including isotropic and subsequently anisotropic displacement parameters for all non-hydrogen nondisordered atoms. Particular details concerning the existence of static disorder and hydrogen refinement are listed in the Supporting Information for this article. All the highest electronic residuals were observed in close proximity to the metals (or in the disordered region) and have no chemical sense.

General Procedure for the Preparation of the [Rh(η^4-diene)-(L_2)][SB_9H_{12}] Salts. All the salts were prepared from the rhodium complexes [RhCl(η^4-diene)]$_2$ (diene = cod, nbd) in either ethanol or methanol under an argon atmosphere. The corresponding ligands bpy, Me_2bpy, phen, and py were added to yellow suspensions of these complexes, affording solutions that were treated with the thiaborane salt $CsSB_9H_{12}$ to yield the precipitation of solids that were then filtered through a frit and subsequently washed with water, ethanol, and ether. Even though cesium chloride is very soluble in water and ethanol, the precipitates could still occlude some CsCl, and therefore, the resulting solids were dissolved in acetone, where CsCl is insoluble, filtered, and evaporated to dryness, affording the organometallic/thiaboranes salts **1**−**8**. The detailed syntheses of the salts are gathered in the Supporting Information for this article.

The NMR properties of the [*arachno*-6-SB_9H_{12}]$^-$ anion do not change through the series of organometallic/thiaborane salts, and for simplicity, we list only the ^{11}B and ^{1}H NRM data of the anion in the salt **1**. The NMR data (virtually identical) of the thiaborane anion in the other salts are gathered in the Supporting Information.

[Rh(η^4-cod)(bpy)][SB_9H_{12}] (1). Yield: 92%. Anal. Calcd for $C_{18}H_{32}N_2RhSB_9$: C, 42.50; H, 6.34; N 5.51, S, 6.30. Found: C, 42.41; H, 6.41; N, 5.80; S, 6.23. IR (KBr, disk): ν 2527 s (BH), 2514 s (BH), 2501 s (BH), 2487 s (BHB), 2463 s (BHB), 2425 s (BHB), 1603 m, 1472 m, 1443 s, 1313 w, 1261 m, 1160 m, 1009 m, 954 m, 864 w, 797 w, 761 s, 727 w, 482 w, 367 w. LRMS (FAB$^+$): *m*/*z* 367 [M]$^+$ (isotope envelope corresponding to the parent ion [Rh(cod)(bpy)]$^+$), 259 [M − cod]$^+$ (isotope envelope). ^{11}B NMR (96 MHz, CD_2Cl_2, 300 K): δ +3.4 (d, 121 Hz, 1BH), −8.5 (d, 148 Hz, 2BH), −11.8 (d, 165 Hz, 1BH), −15.9 (t, 110 Hz, 1BH_2), −34.0 (d, 134 Hz, 2BH), −37.0 (d, 139 Hz, 2BH). ^{1}H NMR (300 MHz, CD_2Cl_2, 300 K): δ 8.18 (m, 4.0 Hz, 4H; $C_{10}H_8N_2$), 7.82 (m, 4.8 Hz, 3H; $C_{10}H_8N_2$), 7.64 (m, 4.7 Hz, 1H; $C_{10}H_8N_2$), 4.57 (m, 4H; vinyllic), 2.70 (s, 1H; BH), 2.59 (m, 4H; allylic), 2.40 (s, 3H; BH), 2.16 (m, 4H; allylic), 1.26 (s, 1H; BH), 0.67 (s, 2H; BH), 0.44 (s, 1H; BH), 0.30 (s, 2H; BH), −1.84 (s, 2H; BHB).

In dichloromethane solution at room temperature, **1** transforms into a mixture of products of which one has been characterized as [8,8-bpy-*nido*-8,7-$RhSB_9H_{10}$] (see below); it is likely that one of the other unisolated species is a complex of an organometallic rhodium fragment with the [SB_9H_{12}]$^-$ anion (see below for compound **5**). The NMR data of the final mixture are as follows. ^{11}B NMR (96 MHz, CD_2Cl_2, 300 K): δ 16.9 (br,), 10.8 (br); 7.3 (br), 5.4 (d 157 Hz), 3.5, d 135 Hz, 2.5 (sh), −6.2 (br), −8.3 (br), −15.9 (d, 159 Hz), −20.3, −21.5, −24.9 (d, 136 Hz), −29.9, −31.8; −37.0; −38.1; −39.3. ^{1}H NMR (300 MHz, CD_2Cl_2, 300 K): δ 8.30−7.63 (aromatic), 4.67 (BH), 4.59 (m, 4H, vinyllic), 3.70 (BH), 3.24 (BH), 3.17 (BH), 3.05 (BH), 2.66 (BH), 2.60 (m, 4H, allylic), 2.55 (BH), 2.39 (BH), 2.16 (m,4H, allylic), 1.76 (BH), 1.57 (BH), 1.50 (strongest), 1.11 (BH), 0.93 (BH), 0.76 (BH), −0.89 (BHB), −1.83 (BHB), −2.50 (BHB).

(16) (a) *SHELXTL Package*, v. 6.10; Bruker AXS: Madison, WI, 2000. (b) Sheldrick, G. M. *SHELXS-86 and SHELXL-97*; University of Göttingen: Göttingen, Germany, 1997.

[Rh(η^4-nbd)(bpy)][SB_9H_{12}] (2). Yield: 90%. The analytically pure product was obtained by crystallization in acetone/ether. Anal. Calcd for $C_{17}H_{28}B_9N_2RhS$: C, 41.44; H, 5.73; N 5.69, S, 6.51. Found: C, 41.11; H, 5.71; N, 5.70; S, 6.29. IR (KBr, disk): ν 2526 vs (BH), 2410 m (shoulder, BH), 1600 m, 1492 w, 1469 m, 1444 s, 1306 w, 1158 w, 1009 m, 762 w, 726 s, 496 w. LRMS: MALDI$^+$, *m*/*z* 351 [M]$^+$ (isotope envelope corresponding to the parent ion [Rh(nbd)(bpy)]$^+$); MALDI$^-$, *m*/*z* 140 [M]$^-$ (isotope envelope corresponding to the parent anion [SB_9H_{12}]$^-$). ^{1}H NMR (300 MHz, CD_2Cl_2, 300 K): δ 8.18 (m, 6.0 Hz, 4H; $C_{10}H_8N_2$), 7.62 (m, 4H; $C_{10}H_8N_2$), 4.43 (m, 2.0 Hz, 4H; vinyllic), 4.14 (s, 2H; nbd), 1.61 (s, 2H; nbd).

[Rh(η^4-cod)(Me_2bpy)][SB_9H_{12}] (3). Yield: 80%. The analytically pure product was obtained by crystallization in acetone/ether. Anal. Calcd for $C_{20}H_{36}B_9N_2RhS$: C, 44.75; H, 6.76; N 5.22, S, 5.97. Found: C, 44.98; H, 6.96; N, 5.15; S, 6.15. IR (KBr, disk): ν 2515 s (BH), 2500 s (BH), 2545 s (BH), 2399 s, 1616 m, 1489 m, 1481 m, 1428 m, 1331 m, 1305 m, 1006 m, 834 m, 787 w, 476 w. LRMS: MALDI$^+$, *m*/*z* 395 (100) [M]$^+$ (isotope envelope corresponding to the parent ion [Rh(cod)(Me_2bpy)]$^+$); MALDI$^-$, *m*/*z* 142 [M]$^-$ (isotope envelope corresponding to the parent ion [SB_9H_{12}]$^-$). ^{1}H NMR (300 MHz, CD_2Cl_2, 300 K): δ 7.98 (s, 2H; $C_{12}H_{12}N_2$), 7.64 (m, 2H; $C_{12}H_8N_2$), 7.40 (m, 2H; $C_{12}H_{12}N_2$), 4.53 (m, 4H; vinyllic), 2.69 (14H; allylic + 2CH_3), 2.14 (m, 4H; allylic).

[Rh(η^4-nbd)(Me_2bpy)][SB_9H_{12}] (4). Yield: 92%. The analytically pure product was obtained by crystallization in acetone/ether. Anal. Calcd for $C_{19}H_{32}B_9N_2RhS$: C, 43.82; H, 6.19; N 5.38, S, 6.16. Found: C, 43.73; H, 5.95; N, 5.26; S, 6.41. IR (KBr, disk): ν 2523 vs (BH), 2463 m (shoulder, BH), 2423 m (shoulder, BH), 1614 s, 1484 w, 1420 m, 1444 s, 1305 m, 1158 w, 1009 m, 827 m, 795 m, 496 w. LRMS: MALDI$^+$, *m*/*z* 379 [M]$^+$ (isotope envelope corresponding to the parent ion [Rh(nbd)Me_2bpy]$^+$); MALDI$^-$, *m*/*z* 140 [M]$^-$ (isotope envelope corresponding to the parent anion [SB_9H_{12}]$^-$). ^{1}H NMR (300 MHz, $(CD_3)_2CO$, 300 K): δ 8.39 (s, 2H; $C_{12}H_{12}N_2$), 7.78−7.76 (m, 2H; $C_{12}H_{12}N_2$), 7.58−7.57 (2H; $C_{12}H_{12}N_2$), 4.58 (m, 2.1 Hz, 4H; vinyllic), 4.12 (br m, 2H; nbd), 2.59 (s, 6H; CH_3), 1.61 (s, 2H; nbd).

[Rh(η^4-cod)(phen)][SB_9H_{12}] (5). Yield: 88%. IR (KBr, disk): ν 2524 vs (BH), 2416 m (shoulder, BH), 2326 w (BHB), 1627 w, 1601 w, 1517 m, 1491 w, 1425 s, 1414 m, 1330 w, 1307 w, 1261 w, 1219 w, 1145 w, 1095 w, 1044 w, 1009 m, 955 w, 911w, 891 w, 874 w, 861 w, 841 s, 815 w, 790 w, 768 w, 746 w, 717 s. 687 w, 645 w, 596 w, 500 w, 491 w, 474 w. LRMS (FAB$^+$): *m*/*z* 391 [M]$^+$ (isotope envelope corresponding to the parent ion [Rh(cod)-(phen)]$^+$), 283 (48) [M − cod]$^+$ (isotope envelope). ^{1}H NMR (300 MHz, CD_2Cl_2, 300 K): δ 8.67 (m, 5.6 Hz, 2H; $C_{12}H_8N_2$), 8.22 (br s, 2H; $C_{12}H_8N_2$), 8.08 (m, 2.4 Hz, 1.0 Hz, 2H; $C_{12}H_8N_2$), 7.95 (m, 2.8 Hz, 2H; $C_{12}H_8N_2$), 4.78 (br s, 4H; vinyllic), 2.65 (m, 4H; allylic), 2.24 (m, 4H; allylic).

In dichloromethane solution at room temperature, **5** transforms into a new boron-containing species that is unstable and has not been isolated as a pure compound. The following NMR data correspond to the transformation mixture, and the assignments are tentative: ^{11}B NMR (96 MHz, $CDCl_3$, 300 K) δ 5.1 (d, 123 Hz, 1BH), −8.2 (d, 117 Hz, 3BH), −11.3 (sh, 1BH), −32.9 (d, 123 Hz, 2BH), −38.0 (d, 146 Hz, 2BH); ^{1}H NMR (400 MHz, $CDCl_3$, 233 K) δ 8.89 (d, 4.2 Hz, 2H), 8.41 (br s), 8.24 (d, 8.2 Hz, 2H), 7.81 (d, 8.5 Hz, 2H), 7.51 (dd, 4.2, 8.2 Hz, 2H), 7.46 (d, 8.5 Hz, 2H), 3.95 (m, 2H, CH), 3.30 (m, 2H, CH2), 3.32 (br s, 1H, BH), 3.17 (m, 4H, CH_2), 3.05 (m, 2H, CH_2), 2.61 (br s, 1H, BH), 2.52 (br s, 1H, BH), 2.27 (br s, 1H, BH), 2.12 (m, 4H, CH_2), 1.10 (br s, 1H, BH), 0.91 (br s, 2H, BH), 0.82 (br s, 2H, BH), 3.27 (BH), 2.63 (BH), 2.52 (BH), 2.42 (BH), 1.89 (BH), 1.45 (BH), 1.37 (BH),

1.23 (BH), 0.92 (BH), 0.80 (BH), 0.64 (BH), 0.22 (BH), −1.97 (br s, 1H, BHB, 1H), −2.50 (br s, 1H, BHB). LRMS (MALDI$^-$): *m*/*z* 176 [M]$^-$ (isotope envelope corresponding to the anion $[SB_9H_{11}Cl]^-$). The results suggest that the new species is a complex of an organometallic fragment of rhodium with a $\{SB_9H_{12}\}$- or $\{SB_9H_{11}Cl\}$-cage.

Additional NMR data such as [^{1}H−^{1}H]-COSY, illustration of the evolution of the ^{1}H and ^{11}B NMR spectra of the salt **5** as function of time, and variable-temperature ^{1}H NMR spectra can be found in the Supporting Information for this article.

[Rh(η^4-nbd)(phen)][SB_9H_{12}] (6). Yield: 95%. The analytically pure product was obtained by crystallization in acetone/ether. Anal. Calcd for $C_{19}H_{28}B_9N_2RhS$: C, 44.16; H, 5.46; N 5.42, S, 6. 21. Found: C, 44.31; H, 5.29; N, 5.43; S, 6.19. IR (KBr, disk): ν 2513 vs (BH), 2420 m (shoulder, BH), 1515 m, 1425 s, 1307 m, 1221 w, 1175 m, 1011 m, 842 s, 717 s. LRMS: MALDI$^+$, *m*/*z* 375 [M]$^+$ (isotope envelope corresponding to the parent ion [Rh(nbd)-(phen)]$^+$); MALDI$^-$, *m*/*z* 140 [M]- (isotope envelope corresponding to the parent anion $[SB_9H_{12}]^-$). ^{1}H NMR (300 MHz, CD_2Cl_2, 300 K): δ 8.65 (d, 8.3 Hz, 2H; $C_{12}H_8N_2$), 8.07 (s, 4H; $C_{12}H_8N_2$), 7.92−7.88 (m, 2H; $C_{12}H_8N_2$), 4.60 (s, 4H; vinyllic), 4.21 (br s, 2H; nbd), 2.59 (s, 6H; CH_3), 1.52 (s, 2H; nbd).

[Rh(η^4-cod)(py)$_2$][SB_9H_{12}] (7). Yield: 79%. IR (KBr, disk): ν 3435 m, 3060 w, 3009 w, 2917 w, 2879 w, 2832 w, 2525 vs (BH), 2404 m (shoulder, BH), 2328 w (BHB), 1601 w, 1482 w, 1446 w, 1430 w, 1239 w, 1207 w, 1175 s, 1064 w, 1042 s, 1006 w, 944 w, 913 w, 893 w, 874 w, 786 s, 752 w, 697 w, 637 w, 591 w, 479 w, 452 w, 358 w, 371 w, 358 w. ^{1}H NMR (300 MHz, CD_2Cl_2, 273 K): δ 8.67 (s, 4H; C_5H_5N), 7.78 (m, 2H; C_5H_5N), 7.40 (m, 6.1 Hz, 4H; C_5H_5N), 4.78 (br s, 4H; vinyllic), 2.65 (m, 4H; allylic), 2.45 (s, 3H, BH), 2.24 (m, 4H; allylic).

[Rh(η^4-nbd)(py)$_2$][SB_9H_{12}] (8). Yields: 74%. IR (KBr, disk): ν 3425 m, 3053 w, 3002 w, 2930 w, 2850 w, 2512 vs (BH), 2343 m (shoulder, BH), 2326 w (BHB), 1600 w, 1484 w, 1445 w, 1403 w, 1303 w, 1212 w, 1174 s, 1064 w, 1043 s, 1007 w, 941 w, 914 w, 798 w, 752 w, 694 w, 637 w, 592 w, 469 w, 450 w, 370 w, 348 w. ^{1}H NMR (300 MHz, CD_3CN, 300 K): δ 8.43 (m, 4H; C_5H_5N), 7.80 (t, 7.6 Hz, 4H; C_5H_5N), 7.36 (m, 6.1 Hz, 4H; C_5H_5N), 3.94 (s, 4H; vinyllic), 3.82 (br s, 2H; nbd), 1.52 (s, 2H; nbd).

Preparation of the Rhodathiaboranes [8,8-(L$_2$)-*nido*-8,7-$RhSB_9H_{10}$]. The rhodathiaboranes containing $\{Rh(L_2)\}$-fragments were obtained directly from the corresponding [Rh(nbd)(L$_2$)]-$[SB_9H_{12}]$ salts, **2**, **4**, and **6** (L$_2$ = bpy, Me$_2$bpy, phen).

In a typical reaction, about 50 mg portions of the salts were dissolved in CH_2Cl_2 under an argon atmosphere and the resulting solutions stirred at room temperature for several hours. After this time, the reaction mixtures were filtered through Celite to give dark red solutions, which were evaporated until dryness, and the resulting residues were crystallized from CH_2Cl_2/hexane to give the 11-vertex *nido*-rhodathiaboranes, **9**−**11**.

Similarly, the cod− and nbd−Rh(I) salts, **7** and **8**, led to the formation of [8,8-(py)$_2$-*nido*-8,7-$RhSB_9H_{10}$] (**12**).

[8,8-(bpy)-*nido*-8,7-$RhSB_9H_{10}$] (9). A 10 mg (0.02 mmol) amount of **2** afforded 6 mg (0.015 mmol, 74%) of **9**. IR (KBr, disk): ν 2957 s, 2924 vs, 2522 (BH), 1740 vw, 1600 w, 1444 m, 1377 m, 1154 sh, 1096 s, 1019 s, 864 m, 800 s, 761 m, 700 w, 658 w. LRMS (MALDI$^-$): *m*/*z* 398 [M − H]$^-$ (isotope envelope corresponding to the parent anion $[C_{10}H_{17}N_2RhSB_9]^-$). ^{11}B NMR (96 MHz, CD_2Cl_2, 300 K): δ 17.7 (br d, 143 Hz, 1B), 11.7 (br d, 147 Hz, 1B), 6.8 (d, 154 Hz, 1B), 2.7 (d, 129 Hz, 2B), −15.2 (d, 140 Hz, 1B), −19.9 (d, 147 Hz, 1B), −22.0 (d, 165 Hz, 1B), −32.3 (br d, 167 Hz, 1BH). ^{1}H NMR (300 MHz, CD_2Cl_2, 300 K): δ 9.45 (s, 1H; $C_{10}H_8N_2$), 9.18 (s, 1H; $C_{10}H_8N_2$), 8.19 (m, 2H; $C_{10}H_8N_2$), 8.07 (m, 2H; $C_{10}H_8N_2$), 7.70 (m, 1H; $C_{10}H_8N_2$), 7.52 (m, 1H; $C_{10}H_8N_2$), 4.79 (s, 1H; BH), 3.70 (s, 1H; BH), 3.39 (s, 1H; BH), 3.23 (s, 1H; BH), 3.14 (s, 1H; BH), 1.82 (s, 1H; BH), 1.61 (s, 1H; BH), 1. 27 (s, 1H; BH), 0.97 (s, 1H; BH), −0.78 (s, 1H; BHB).

[8,8-(Me$_2$bpy)-*nido*-8,7-$RhSB_9H_{10}$] (10). A 15 mg (0.02 mmol) amount of **4** gave 8.9 mg of **10** (0.021 mmol; 72%). Anal. Calcd for $C_{12}H_{22}B_9N_2RhS$: C, 33.79; H, 5.20; N 6.57, S, 7.52. Found: C, 33.64; H, 5.15; N, 6.39; S, 7.48. IR (KBr, disk): ν 2923 s, 2853 s, 2518 vs (BH), 1735 vw, 1615 s, 1556 w, 1443 s, 1378 s, 1261 m, 1216 w, 1095 m, 1021 s, 922 w, 823 s, 802 s, 732 w, 700 w, 551 w, 517 m. LRMS (MALDI$^-$): *m*/*z* 427 [M]$^-$ (isotope envelope corresponding to the parent anion $[C_{12}H_{22}N_2RhSB_9]^-$). ^{11}B NMR (96 MHz, $CDCl_3$, 300 K): δ 18.8 (v br s, 1B), 12.3 (v br, 1B), 7.1 (v br, 1B), 2.3 (d, 140 Hz, 2B), −15.2 (d, 139 Hz, 1B), −19.3 (d, 150 Hz, 1B), −21.7 (br d, 122 Hz, 1B), −32.2 (v br, 1B). ^{1}H NMR (300 MHz, $CDCl_3$, 300 K): δ 9.28 (d, 5.4 Hz, 1H; $C_{12}H_{12}N_2$), 8.50 (d, 5.4 Hz, 1H; $C_{12}H_{12}N_2$), 7.92 (s, 1H; $C_{12}H_{12}N_2$), 7.81 (s, 1H; $C_{12}H_{12}N_2$), 7.46 (m, 1H; $C_{12}H_{12}N_2$), 7.27 (m, 1H; $C_{12}H_{12}N_2$), 4.82 (s, 1H; BH), 3.87 (s, 1H; BH), 3.52 (s, 1H; BH), 3.27 (s, 1H; BH), 3.22 (sh, 1H; BH), 2.62 (s, 3H; CH_3), 2.54 (s, 3H; CH_3), 1.95 (s, 1H; BH), 1.77 (s, 1H; BH), 1.41 (s, 1H; BH), 1.00 (s, 1H; BH), −0.64 (s, 1H; BHB).

[8,8-(phen)-*nido*-8,7-$RhSB_9H_{10}$] (11). A 10 mg (0.019 mmol) anount of **6** gave 4.2 mg of **11** (0.0099 mmol; 51%). IR (KBr, disk): ν 2962 m, 2850 m 2514 vs (BH), 1630 w, 1598 w, 1577 w, 1514 m, 1495 w, 1424 s, 1387 m, 1302 w, 1261 s, 1088 vs, 1018 vs, 840 s, 799 s, 718 s, 689 m. LRMS (MALDI$^-$): *m*/*z* 423 [M]$^-$ (isotope envelope corresponding to the parent anion $[C_{12}H_{18}N_2RhSB_9]^-$). ^{11}B NMR (96 MHz, CD_2Cl_2, 300 K): δ 18.8 (br d, 135 Hz, 1B), 12.8 (br d, 146 Hz, 1B), 7.2 (d, 133 Hz, 1B), 4.4 (d, 166 Hz, 1B), 2.6 (d, 137 Hz, 1B), −15.1 (d, 143 Hz, 1B), −19.2 (d, 142 Hz, 1B), −21.8 (d, 155 Hz, 1B), −33.0 (br, 1BH). ^{1}H NMR (300 MHz, CD_2Cl_2, 300 K): δ 9.72 (s, 1H; $C_{12}H_8N_2$), 9.47 (s, 1H; $C_{12}H_8N_2$), 8.62 (m, 2H; $C_{12}H_8N_2$), 8.50 (m, 2H; $C_{12}H_8N_2$), 8.02 (m, 1H; $C_{12}H_8N_2$), 7.82 (m, 1H; $C_{12}H_8N_2$), 5.33 (s, 1H; BH), 3.93 (s, 1H; BH), 3.72 (s, 1H; BH), 3.48 (s, 1H; BH), 3.39 (s, 1H; BH), 2.04 (s, 1H; B H), 1.89 (s, 1H; BH), 1.48 (s, 1H; BH), 1.11 (s, 1H; BH), −0.36 (s, 1H; BHB).

[8,8-(py)$_2$-*nido*-8-,7-SB_9H_{10}] (12). ^{11}B NMR (96 MHz, CD_2Cl_2, 300 K): δ 17.7 (br, 1B), 12.5 (br d, 136 Hz, 1B), 6.9 (d, 142 Hz, 1B), 2.0 (d, 128, 2B), −15.3 (d, 143 Hz, 1B), −20.8 (d, 134 Hz, 1B), −22.2 (br, 1B), −33.1 (br, 1B). ^{1}H NMR (300 MHz, CD_2Cl_2, 273 K): 8.42 (m, 4H; C_5NH_5), 7.97 (m, 1H; C_5NH_5), 7.78 (m, 1H; C_5NH_5), 7.52 (m, 3H; C_5NH_5), 7.31 (m, 1H; C_5NH_5), 4.89 (s, 1H; BH), 3.66 (s, 1H; BH), 3.42 (s, 1H; BH), 2.91 (s, 1H; BH), 2.77 (s, 1H; BH), 1.66 (s, 1H; BH), 1.55 (s, 1H; BH), 1.47 (s, 1H; BH), 1.38 (s, 1H; BH), −0.70 (s, 1H, BHB).

In contrast, the cod−Rh salts **1** and **3** yield mixtures of the *nido*-rhodathiaboranes, **9** and **10**, together with new uncharacterized species. Under the same conditions, **5** affords a single boron-containing compound, which, on the basis of NMR data deposited in the Supporting Information, we propose as an *exo*-plolyhedral rhodium/thiaborane complex.

[8,8-(L$_2$)-8-(PPh_3)-*nido*-8,7-$RhSB_9H_{10}$] (L$_2$ = bpy, Me$_2$bpy, phen). These 11-vertex *nido*-rhodathiaboranes can be obtained from reactions between the salts **1**−**4** and **6** and triphenylphosphine in a hydrogen atmosphere at room temperature. The nbd−Rh salts react faster than their cod−Rh congeners and afford higher yields. In contrast, the cod−Rh salt **5** affords the rhodium dihydride [Rh-(phen)(PPh_3)$_2$(H)$_2$]$^+$ under the same conditions (see below).

As reported above, the nbd-containing reagents **2**, **4**, and **6** lead to the formation of the corresponding [8,8-(L$_2$)-*nido*-8,7-$RhSB_9H_{10}$] clusters; thus, *nido*-rhodathiaboranes incorporating $\{(L_2)(PPh_3)Rh\}$

moieties can be alternatively prepared from CH_2Cl_2 solutions of the nbd−Rh salts and triphenylphosphine. However, the salts **1**, **3**, and **5** do not provide convenient synthetic routes to the PPh_3-ligated *nido*-rhodathiaboranes, **13**−**15**, in the absence of molecular hydrogen as the cod−Rh reagents yield mixtures of the {Rh(L$_2$)}−*nido*-rhodathiaboranes and new uncharacterized compounds in CH_2Cl_2. The synthetic details of **13**−**15** are included in deposited material.

[8,8-(bpy)-8-(PPh$_3$)-*nido*-8,7-RhSB$_9$H$_{10}$] (13). Yield: 60%. IR (KBr, disk): ν 3110 w, 3081 w, 3057 w, 2963 w, 2925 w, 2852 w, 2558 sh (BH), 2505 vs (BH), 1598 m, 1573 w, 1480 m, 1469 m, 1443 s, 1432 s, 1312 m, 1261 s, 1175 w, 1159 w, 1094 s, 1020 s, 1007 s, 865 w, 802 m, 759 s, 750 s, 698 s, 630 w, 528 s, 488 m, 461 w. LRMS (EI): *m*/*z* 661 [M]$^+$ (isotope envelope corresponding to the parent ion [$C_{28}H_{33}B_9N_2P_1Rh_1S_1$]$^+$). ^{11}B NMR (96 MHz, acetone-d_6, 300 K): δ 10.8 (br, 2B), 5.9 (br, 2B), −3.8 (br, 1B), −18.7 (d, 134 Hz, 2B), −23.0 (br, 1B), −30.9 (br, 1B). ^{1}H NMR (300 MHz, acetone-d_6, 300 K): δ 9.51 (m, 1H; $C_{10}H_8N_2$), 9.09 (m, 1H; $C_{10}H_8N_2$), 8.25 (m, 2H; $C_{10}H_8N_2$), 8.11 (m, 1H; $C_{10}H_8N_2$), 8.00 (m, 1H; $C_{10}H_8N_2$), 7.77 (m, 2H; $C_{10}H_8N_2$), 7.35 to 7.23 (m, 15H; PPh_3), 4.21 (s, 1H; BH), 3.91 (s, 1H; BH), 3.82 (s, 1H; BH), 2.64 (s, 1H; BH), 2.59 (s, 1H; BH), 1.81 (s, 1H; BH), 1.53 (s, 2H; BH), 1.01 (s, 1H; BH), −2.13 (s, 1H; BHB). ^{31}P{^{1}H} NMR (121 MHz, acetone-d_6, 300 K): 35.5 [d, ^1J(^{103}Rh−^{31}P) = 145 Hz, PPh_3].

[8,8-(Me$_2$bpy)-8-(PPh$_3$)-*nido*-8,7-RhSB$_9$H$_{10}$] (14). Yield: 60%. Anal. Calcd for $C_{30}H_{37}N_2B_9PRhS$: C, 52.31; H, 5.41; N 4.07, S, 4.65. Found: C, 52.48; H, 5.30; N, 3.99; S, 4.70. IR (KBr, disk): ν 3050 m, 2915 w, 2516 vs (BH), 1692 w, 1613 m, 1480 m, 1433 s, 1258 w, 1091 m, 1008 m, 917 w, 824 m, 742 s, 696 vs, 532 s. LRMS (MALDI$^+$): *m*/*z* 689 [M]$^-$ (isotope envelope corresponding to the parent anion [$C_{30}H_{37}N_2PRhSB_9$]$^+$). ^{11}B NMR (96 MHz, CD_2Cl_2, 300 K): δ 10.5 (br d, 2B), 5.7 (br, 2B), 6.4 (br, 1B), −3.5 (br, 2B), −19.1 (d, 135 Hz, 1B), −23.1 (d, 138 Hz, 1B), −31.2 (br, 1B). ^{1}H NMR (300 MHz, CD_2Cl_2, 300 K): δ 9.28 (s, 1H; $C_{12}H_{12}N_2$), 8.80 (s, 1H; $C_{12}H_{12}N_2$), 7.58−7.17 (19H; PPh_3 + $C_{12}H_{12}N_2$), 4.16 (s, 1H; BH), 3.71 (s, 2H; BH), 2.53 (s, 1H; BH), 2.49 (s, 3H; CH_3), 2.40 (s, 3H; CH_3), 1.67 (s, 1H; BH), 1.44 (s, 1H; BH), 1.34 (s, 1H; BH), 0.96 (s, 1H; BH), 0.85 (s, 1H; BH), −2.22 (s, 1H; BHB). ^{31}P{^{1}H} NMR (121 MHz, CD_2Cl_2, 300 K): 35.3 [d, ^1J(^{103}Rh−^{31}P) = 146 Hz, PPh_3].

[8,8-(phen)-8-(PPh$_3$)-*nido*-8,7-RhSB$_9$H$_{10}$] (15). Yield: 61%. Anal. Calcd for $C_{30}H_{33}B_9N_2PRhS$: C, 52.61; H, 4.86; N 4.09, S, 4.68. Found: C, 52.46; H, 5.15; N, 3.98; S, 4.68. LRMS: MALDI$^+$, *m*/*z* 685 [M]$^+$ (isotope envelope corresponding to the parent anion [$C_{30}H_{33}N_2PRhSB_9$]$^+$); MALDI$^-$, *m*/*z* 423 [M − PPh_3]$^-$ (isotope envelope). ^{11}B NMR (96 MHz, CD_3CN, 300 K): δ10.5 (br d, 129 Hz, 2B), 5.6 (br s, 129 Hz, 2B), −4.3 (v br d, 1B), −19.3 (d, 144 Hz, 2B), −23.7 (d, 139 Hz, 1B), −31.2 (br, 1B). ^{1}H NMR (300 MHz, CD_3CN, 300 K): δ 9.74 (1H; $C_{12}H_8N_2$), 9.28 (1H; $C_{12}H_8N_2$), 8.38 (1H; $C_{12}H_8N_2$), 8.26 (1H; $C_{12}H_8N_2$), 7.92 (m, 1H; $C_{12}H_8N_2$), 7.78 (m, 3H; $C_{12}H_8N_2$), 7.11−6.99 (m, 15H; PPh_3), 4.87 (s, 1H; BH), 3.85 (s, 1H; BH), 3.76 (s, 1H; BH), 2.72 (s, 1H; BH), 2.50 (s, 1H; BH), 1.75 (s, 1H; BH), 1.48 (s, 1H; BH), 1.31 (s, 1H; BH), 0.97 (s, 1H; BH), −2.02 (s, 1H; BHB). ^{31}P{^{1}H} NMR (121 MHz, CD_3CN, 300 K): 35.6 [d, ^1J(^{103}Rh−^{31}P) = 145 Hz, PPh_3].

[8,8-(bpy)-8-(NCCH$_3$)-*nido*-8,7-RhSB$_9$H$_{10}$] (16). This compound is formed when the rhodathiaborane **9** is dissolved in CH_3CN. LRMS (MALDI$^-$; DCTB matrix): *m*/*z* 646 [M − $NCCH_3$ − 3H + DCTB]$^-$, 491 [M − $NCCH_3$ − 2H − bpy + DCTB]$^-$, 437 [M − 3H]$^-$, 398 [M − H − $NCCH_3$]$^-$, 278 [M − bpy − 6H]$^-$ (the match between experimental and calculated isotope patterns is good for all the anions). ^{11}B NMR (96 MHz, CD_3CN, 300 K): δ12.0 (br, 1B), 9.1 (1B), 8.3 (1B), 3.1 (d, 127 Hz, 1B), −4.6 (d, 146 Hz, 1B), −19.6 (d, 133 Hz, 2B), −23.7 (d, 136 Hz, 1B), −31.9 (br d, 145 Hz, 1B). ^{1}H NMR (300 MHz, CD_3CN, 300 K): δ 9.01 (d, 5.1 Hz, 1H; $C_{10}H_8N_2$), 8.90 (d, 5.1 Hz, 1H; $C_{10}H_8N_2$), 8.38 (d, 8.0 Hz, 1H; $C_{10}H_8N_2$), 8.03 (t, 8.0 Hz, 1H; $C_{10}H_8N_2$), 8.16 (t, 7.6 Hz, 1H; $C_{10}H_8N_2$), 8.03 (t, 7.0 Hz, 1H; $C_{10}H_8N_2$), 7.72 (t, 5.8 Hz, 1H; $C_{10}H_8N_2$), 7.50 (t, 6.3 Hz, 1H; $C_{10}H_8N_2$), 4.09 (s, 1H; BH), 3.68 (s, 1H; BH), 3.32 (s, 1H; BH), 3.32 (s, 1H; BH), 2.08 (s, 1H; BH), 1.37 (s, 3H; BH), 0.72 (s, 1H; BH), −2.37 (s, 1H; BHB). ^{13}C NMR (300 MHz, CD_3CN, 300 K): δ 156.77 (s, C_{quart}, bpy), 155.11 (s, C_{quart}, bpy), 15513 (s, CH, bpy), 150.04 (s, CH, bpy), 138.85 (s, CH, bpy), 138.48 (CH, bpy), 126.13 (CH, bpy), 125.25 (CH, $C_{10}H_8N_2$), 123.07 (s, CH, bpy).

[8,8-(Me$_2$bpy)-8-(NCCH$_3$)-*nido*-8,7-RhSB$_9$H$_{10}$] (17). This was obtained from **10** in CH_3CN. LRMS (MALDI$^-$; DCTB matrix): *m*/*z* 491 [M − Me_2bpy − $NCCH_3$ − 2H + DCTB]$^-$, 426 [M − $NCCH_3$ − H]$^-$, 278 [M − Me_2bpy − 6H]$^-$ (the match between experimental and calculated isotope patterns is good for all the anions). ^{11}B NMR (96 MHz, CD_3CN, 300 K): δ 17.3 (br, 1B), 14.3 (2B), 8.3 (1B), 0.7 (d, 127 Hz, 1B), −14.1 (d, 166 Hz, 2B), −18.5 (d, 137 Hz, 1B), −26.5 (d, 130 Hz, 1B). ^{1}H NMR (300 MHz, CD_3CN, 300 K): δ 8.85 (d, 5.3 Hz, 1H; $C_{12}H_{12}N_2$), 8.77 (d, 5.1 Hz, 1H; $C_{12}H_{12}N_2$), 8.27 (s, 1H; $C_{12}H_{12}N_2$), 8.16 (s, 1H; $C_{12}H_{12}N_2$), 7.58 (d, 4.7 Hz, 1H; $C_{12}H_{12}N_2$), 7.37 (d, 5.3 Hz, 1H; $C_{12}H_{12}N_2$), 4.14 (s, 1H; BH), 3.68 (s, 1H; BH), 3.32 (s, 1H; BH), 2.59 (s, 1H; BH), 2.58 (s, 3H; CH_3), 2.52 (s, 3H; CH_3), 2.03 (s, 1H; BH), 1.35 (s, 2H; BH), 1.25 (s, 1H; BH), 0.74 (s, 1H; BH), −2.35 (s, 1H; BHB).

[8,8-(phen)-8-(NCCH$_3$)-*nido*-8,7-RhSB$_9$H$_{10}$] (18). This was obtained from **11** in CH_3CN. LRMS (MALDI$^-$; DCTB matrix): *m*/*z* 491 [M − phen − $NCCH_3$ − 2H + DCTB]$^-$, 423 [M − $NCCH_3$]$^-$, 278 [M − phen − 6H]$^-$ (the match between experimental and calculated isotope patterns is good for all the anions). ^{11}B NMR (96 MHz, CD_3CN, 300 K): δ 12.2 (br, 1B), 9.6 (2B), 8.5 (1B), 3.5 (d, 130 Hz, 1B), −4.2 (d, 141 Hz, 1B), −19.8 (d, 166 Hz, 2B), −23.1 (d, 138 Hz, 1B), −31.9 (d, 130 Hz, 1B). ^{1}H NMR (300 MHz, CD_3CN, 300 K): δ 9.34 (m, 1H; $C_{12}H_8N_2$), 9.24 (m, 1H; $C_{12}H_8N_2$), 8.07 (m, 1H; $C_{12}H_8N_2$), 8.60 (m, 1H; $C_{12}H_8N_2$), 8.06 (m, 3H; $C_{12}H_8N_2$), 7.84 (m, 1H; $C_{12}H_8N_2$), 4.70 (s, 1H; BH), 3.76 (s, 1H; BH), 2.68 (s, 1H; BH), 2.40 (s, 1H; BH), 1.43 (s, 2H; BH), 1.39 (s, 1H; BH), 0.76 (s, 1H; BH), −2.02 (s, 1H; BHB).

Rhodium Dihydride Salts [Rh(H)$_2$(bpy)(PPh$_3$)$_2$][SB$_9$H$_{12}$] (19). Method A. A suspension of $[RhCl(cod)]_2$ (40.0 mg, 0.08 mmol) was treated with 25.3 mg (0.16 mmol) of bipyridine dissolved in methanol to give a bright-red solution. Then, 170 mg (0.65 mmol) of PPh_3 dissolved in ether was added, and the reaction mixture was stirred under hydrogen atmosphere for 2 days. The resulting orange solution was treated with an aqueous $CsSB_9H_{12}$ solution (44.5 mg; 0.162 mmol), causing the formation of an orange precipitate, which was filtered out in air and washed with methanol and water: yield 109 mg (72%). Analytically pure compound was obtained by crystallization in CH_2Cl_2/hexane. Anal. Calcd for $C_{46}H_{52}B_9N_2PRhS{\cdot}2CH_2Cl_2$: C, 52.55; H, 5.15; N 2.55. Found: C, 52.70; H, 4.78; N, 2.36. IR (KBr, disk): ν 3054 w, 2923 w, 2853 w, 2526 vs (BH), 2441 m (BH), 2419 m (BH), 2098 sh (Rh−H), 2072 m (Rh−H), 1598 m, 1467 m, 1479 m, 1434 s, 1384 w, 1261 w, 1182 m, 1159 m, 1119 m, 1094 s, 1044 w, 1011 m, 971 w, 915 w, 746 s, 694 vs, 587 w, 540 m, 520 vs, 500 m, 452 w, 361 w. MS (FAB$^+$, *m*/*z* (%)): 785 (82) [M]$^+$ (isotope envelope corresponding to the parent ion [Rh(bpy)(PPh_3)$_2$(H)$_2$]$^+$), 521 [M − PPh_3 − 2H]$^+$, 441 [M − PPh_3 − 2H − Ph]$^+$, 366 [M − PPh_3 − 2H − 2Ph]$^+$, 259 [M − 2PPh_3 − 2H]$^+$ (isotope envelopes). ^{1}H NMR (300 MHz, $CDCl_3$, 300 K): δ 8.05 (d, 2H; $C_{10}H_8N_2$), 7.96 (d, 2H; $C_{10}H_8N_2$), 7.79 (t, 2H; $C_{10}H_8N_2$), 7.56 (d, 1H; PPH_3), 7.49 (m, 2H; PPh_3), 7.35 (m, 27 H; PPh_3), 6.79 (t, 2H; $C_{10}H_8N_2$), −15.66 (apparent q,

Scheme 1

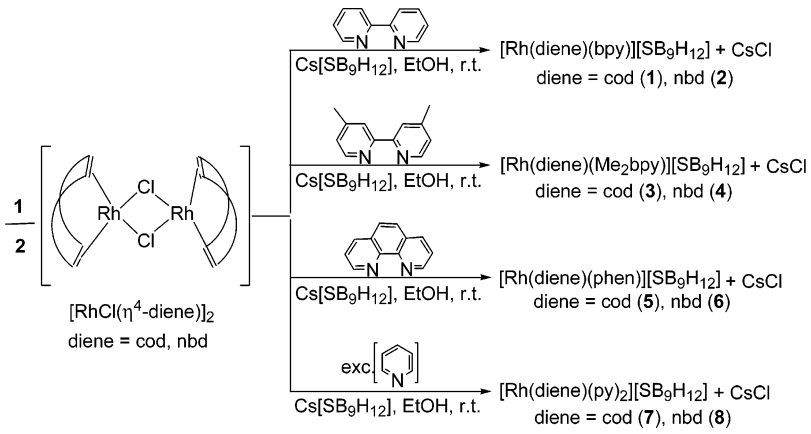

$^1J(^{103}Rh-^1H) \approx {}^2J(^{31}P-^1H) = 15$ Hz, 2H; Rh−H, {^{31}P}, d, $^1J(^{103}Rh-^1H) = 15$ Hz). $^{31}P\{^1H\}$ NMR (121 MHz, $CDCl_3$, 300 K): δ 47.7 [d, $^1J(^{103}Rh-^{31}P) = 114$ Hz, PPh_3].

Method B. A 0.016 g (0.062 mmol) amount of PPh_3 dissolved in Et_2O was added to a suspension of 0.033 g (0.062 mmol) of the salt [Rh(cod)bpy][SB_9H_{12}] (**1**) in MeOH. The system was cooled to the temperature of liquid nitrogen, and then, a balloon attached to the Scklenk tube and containing hydrogen gas was opened. The reaction mixture was vigorously stirred from low to room temperature, and the stirring, under a hydrogen atmosphere, was maintained for 2 days. After this time, a brown solution and a yellow precipitate were formed. Filtration through a filter stick afforded an orange solution and a brown precipitate. The orange filtrate was evaporated to dryness and crystallized from dichloromethane/hexane to give 0.005 g of the rhodium dihydride salt **19** (16%).

Method C. A 0.035 g (0.0069 mmol) amount of **1** was treated with 0.073 g (0.27 mmol) of PPh_3 in methanol. The reactants were stirred for 6 days at room temperature under argon atmosphere. After this time, NMR spectroscopy of the mixture demonstrated formation of the rhodium dihydride complex in small concentration, together with the starting $[Rh(cod)bpy]^+$ cation. This route, therefore, is not a good method for the preparation of **19**, but it demonstrates that there is formation of the dihydride (in very small amount) in the absence of molecular hydrogen.

[Rh(H)$_2$(Me$_2$bpy)(PPh$_3$)$_2$][SB$_9$H$_{12}$] (20). The procedure was similar to method A above but starts from the nbd complex, $[RhCl(nbd)]_2$ (40 mg; 0.09 mmol). The hydrogenation of the nbd ligand is faster than that of the cod; thus, the reaction with PPh_3 in hydrogen atmosphere is completed in 4 h. Subsequent addition of the thiaborane salt affords **20** (64 mg; 0.07 mmol; 40%). ^1H NMR (300 MHz, $CDCl_3$, 300 K): δ 7.87−6.56 (36H, PPh_3 + Me_2bpy), 2.45 (s, 6H; CH_3), −15.78 (apparent q, $^1J(^{103}Rh-^1H) \approx {}^2J(^{31}P-^1H) = 14$ Hz, 2H; Rh−H, {^{31}P}, d, $^1J(^{103}Rh-^1H) = 15$ Hz). $^{31}P\{^1H\}$ NMR (121 MHz, $CDCl_3$, 300 K): δ 47.3 [d, $^1J(^{103}Rh-^{31}P) = 115$ Hz, PPh_3].

[Rh(H)$_2$(phen)(PPh$_3$)$_2$][SB$_9$H$_{12}$] (21). Method A. A 32 mg (0.18 mmol) amount of phenanthroline was added, dissolved in methanol, to a suspension of $[RhCl(cod)]_2$ (40 mg, 0.08 mmol) in MeOH. The resulting bright red solution was treated with 170 mg (0.6488 mmol) of triphenylphosphine in ether, and the reaction mixture was stirred under hydrogen atmosphere (balloon attached to the Schlenk tube) for 2 days. Addition of $CsSB_9H_{12}$ (44.5 mg, 0.16 mmol) dissolved in H_2O cause the precipitation of **21**, which was filtered out in air, washed with methanol/water, and dried in vacuum (110 mg, 72%). LRMS (FAB^+): *m*/*z* 809 $[M]^+$ (isotope envelope corresponding to the parent anion $[Rh(phen)(PPh_3)(H)_2]^+$), 545 [M − PPh_3 − 2H]$^+$, 468 [M − PPh_3 − 2H − Ph]$^+$, 391 [M − PPh_3 − 2H − 2Ph]$^+$, 283 [M − 2PPh_3 − 2H]$^+$ (isotope envelopes). ^{11}B NMR (96 MHz, $CDCl_3$, 300 K): δ +3.9 (d, 136 Hz, 1BH), −8.3 (d, 148 Hz, 2BH), −11.3 (d, 165 Hz, 1BH), −16.1 (t, 105 Hz, 1BH_2), −37.0 (d, 137 Hz, 2BH), −33.7 (d, 140 Hz, 2BH). ^1H NMR (300 MHz, $CDCl_3$, 300 K): δ 8.47 (m, 2H, $C_{12}H_8N_2$), 8.31 (d, 2H, $C_{12}H_8N_2$), 7.92 (d, 2H, $C_{12}H_8N_2$), 7.67 (m, 2H, $C_{12}H_8N_2$), 7.46 (m, 30H, PPh_3), 3.05 (s, 1H, BH), 2.77 (s, 2H, BH), 2.62 (s, 1H, BH), 2.13 (s,1H, BH), 1.55 (s, 2H, BH), 0.96 (s,1H, BH), 0.66 (s, 2H, BH), −1.60 (s, 2H, BHB), −15.30 (apparent q, $^1J(^{103}Rh-^1H) \approx {}^2J(^{31}P-^1H) = 15$ Hz, 2H; Rh−H, {^{31}P}, d, $^1J(^{103}Rh-^1H) = 16$ Hz). ^{31}P NMR (121 MHz, $CDCl_3$, 300 K): 48.4 [d, $^1J(^{103}Rh-^{31}P) = 114$ Hz, PPh_3].

Rhodium Carbonyl Salts [Rh(CO)(L$_2$)(PPh$_3$)$_2$][SB$_9$H$_{12}$]. The reactions of the salts **1**−**6** with CO(g) in the presence of PPh_3 afforded the corresponding organometallic/thiaborane salts **22**−**24**. Details of the synthetic procedures are reported in the Supporting Information of this article.

[Rh(CO)(bpy)(PPh$_3$)$_2$][SB$_9$H$_{12}$] (22). Yield: 48%. IR (KBr, disk): ν 3061 w, 2956 w, 2521 s (BH), 2444 m (BH), 1938 vs (CO), 1419 s, 1094 s, 689 s, 519 s. LRMS (FAB^+): *m*/*z* 811 $[M^+]$ (isotope envelope corresponding to the parent anion Rh(bpy)(PPh_3)-(CO)]$^+$, 549 [M − PPh_3]$^+$, 521 [M − PPh_3 − CO] $^+$, 441 [M − 2PPh_3 − CO − Ph]$^+$, 366 [M − 2PPh_3 − CO − 2Ph]$^+$, 259 [M − 2PPh_3 − CO]$^+$ (isotope envelops). ^1H NMR (300 MHz, $CDCl_3$, 300 K): δ 8.83 (d, 2H; $C_{10}H_8N_2$), 7.66 (t, 2H; $C_{10}H_8N_2$), 7.432 (m,30H; PPH_3), 7.19 (t, 2H, $C_{10}H_8N_2$). ^{13}C NMR (300 MHz, CD_2Cl_2, 300 K): δ 193.3 (d, ^1J (^{103}Rh, ^{13}C) = 79 Hz, C−O), 152.78 (*o*-C_{quart}, $C_{10}H_8N_2$), 151.94 (*o*-CH, $C_{10}H_8N_2$), 139.003 (*p*-CH, $C_{10}H_8N_2$), 134.16 (CH, PPh_3), 131.480 (CH, PPh_3), 131.16 ($C_{quart,}$ PPh_3), 129.32 (CH, PPh_3), 126.07 (*m*-CH, $C_{10}H_8N_2$), 123.17 (*m*-CH, $C_{10}H_8N_2$). ^{31}P NMR (121 MHz, $CDCl_3$, 233 K): δ 41.7 [d, $^1J(^{103}Rh-^{31}P) = 115$ Hz, PPh_3]. ^{31}P NMR (121 MHz, $CDCl_3$, 300 K): δ 39.3 (br s, coupling not observed).

[Rh(CO)(Me$_2$bpy)(PPh$_3$)$_2$][SB$_9$H$_{12}$] (23). Yield: 68%. Anal. Calcd for $C_{49}H_{54}B_9N_2OP_2RhS$: C, 59.98; H, 5.55; N 2.86, S, 3.27. Found: C, 59.88; H, 5.09; N, 2.82; S, 3.57. IR (KBr, disk): ν 3054 w, 2518 vs (BH), 2416 s (BH), 1930 vs (CO), 1612 s, 1479 s, 1434 s, 1092 s, 1009 m, 826 m, 744 m, 694 s, 517 vs ^1H NMR (300 MHz, $CDCl_3$, 300 K): δ 8.57 (2 H, s, $C_{12}H_{12}N_2$), 8.41 (2 H, s, $C_{12}H_{12}N_2$), 7.60 (2 H, s, $C_{12}H_{12}N_2$), 7.27 (30 H, m, PPh_3), 2.33 (s, 6H; CH_3). ^{31}P NMR (121 MHz, $CDCl_3$, 233 K): 40.5 [d, $^1J(^{103}Rh-^{31}P) = 114$ Hz, PPh_3]; ^{31}P NMR (121 MHz, $CDCl_3$, 300 K): 38.0 (br s, coupling not observed).

[Rh(CO)(phen)(PPh$_3$)$_2$][SB$_9$H$_{12}$] (24). Yield: 49%. IR (KBr, disk): ν 3059 w, 2963 w, 2522 s (BH), 2405 m (BH), 1918 m

Table 1. Experimental X-ray Diffraction Parameters and Crystal Data for [Rh(cod)(bpy)][SB_9H_{12}] (**1**), [Rh(cod)(Me_2bpy)][SB_9H_{12}] (**3**), [8,8-(bpy)-8-(PPh_3)-*nido*-8,7-$RhSB_9H_{10}$] (**13**), [Rh(H_2)(bpy)(PPh_3)$_2$][SB_9H_{12}] (**19**), and [Rh(CO)(PPh_3)$_2$(phen)][SB_9H_{12}] (**24**)

param	**1**	**3**	**13**	**19**	**24**
empirical formula	$C_{18}H_{30}B_9N_2RhS$	$C_{20}H_{36}B_9N_2RhS$	$C_{28}H_{33}B_9N_2PRhS\cdot C_4H_{10}O$	$C_{46}H_{52}B_9N_2P_2RhS\cdot C_2Cl_2\cdot 1/2C_6H_{14}$	$C_{49}H_{50}B_9N_2OP_2RhS\cdot CH_2Cl_2$
mol wt	508.72	536.77	734.91	1055.11	1062.04
cryst dimens (mm)	0.06 × 0.11 × 0.24	0.06 × 0.11 × 0.12	0.04 × 0.14 × 0.23	0.11 × 0.21 × 0.21	0.11 × 0.11 × 0.22
cryst system	monoclinic	orthorhombic	monoclinic	monoclinic	monoclinic
space group	$P2_1/n$	$Pca2_1$	$P2_1/c$	$P2_1/n$	$P2_1/n$
a, Å	7.4908(6)	26.7940(12)	10.837(5)	15.1261(7)	14.9411(7)
b, Å	31.049(3)	12.5915(6)	15.444(5)	18.0842(9)	17.2273(8)
c, Å	10.2626(9)	14.7508(7)	22.495(5)	19.6204(9)	20.9301(9)
β, deg	103.560(2)		101.733(5)	100.4770(10)	108.4090(10)
V, Å^3	2320.4(4)	4976.6(4)	3686(2)	5277.6(4)	5111.6(4)
Z	4	8	4	4	4
D(calcd) (g cm^{-3})	1.456	1.433	1.324	1.328	1.380
μ(Mo Kα) (mm^{-1})	0.836	0.783	0.592	0.562	0.582
$2\theta_{max}$ (deg)	57.8	56.6	57.5	57.8	57.8
transmissn factors	0.827, 0.952	0.798, 0.950	0.874, 0.977	0.889, 0.941	0.880, 0.940
no. of reflcns collcd	12 878	60549	24 289	64 961	62 931
no. of indp reflcns	5492	12 152	8782	12 978	12 574
no. of reflcns obsd [$I > 2\sigma(I)$]	4381	10 316	5890	10 338	9932
no. of params refined	388	631	554	828	806
R	0.0388	0.0419	0.0597	0.0562	0.0576
R_w	0.0906	0.0827	0.1569	0.1348	0.1162
goodness of fit	1.034	1.05	1.027	1.070	1.117

Table 2. Selected Interatomic Lengths (Å) and Angles (deg) for [Rh(cod)(bpy)][SB_9H_{12}] (**1**) and [Rh(cod)(Me_2bpy)][SB_9H_{12}] (**3**)

param	**1**	**3**	param	**1**	**3**
Rh(1)−N(1)	2.102(2)	2.092(3)	N(1)−C(1)	1.342(4)	1.352(5)
Rh(1)−N(2)	2.089(2)	2.087(3)	N(1)−C(5)	1.354(4)	1.356(5)
Rh(1)−C(11)	2.130(3)	2.129(4)	N(2)−C(6)	1.353(4)	1.353(5)
Rh(1)−C(12)	2.138(3)	2.153(4)	N(2)−C(10)	1.348(4)	1.355(5)
Rh(1)−C(15)	2.119(3)	2.118(4)	C(11)−C(12)	1.388(5)	1.382(6)
Rh(1)−C(16)	2.140(3)	2.146(4)	C(15)−C(16)	1.390(5)	1.395(6)
S(6)−B(av)	1.935(4)	1.954(5)	BB(av)	1.811(6)	1.859(6)
B(2)−B(5)	1.886(5)	1.907(6)	B(4)−B(8)	1.761(6)	1.737(6)
B(2)−B(7)	1.874(6)	1.886(6)	B(4)−B(10)	1.762(5)	1.727(6)
B(9)−B(10)	1.939(9)	1.932(8)	B(8)−B(9)	1.920(8)	1.908(6)
B(9)−B(4)	1.724(8)	1.742(6)	B(5)−S(6)−B(7)	99.17(18)	98.3(2)
N(1)−Rh(1)−N(2)	78.60(9)	79.06(11)	B(2)−B(1)−B(3)	59.1(2)	59.1(2)
B(2)−S(6)−B(5)	58.65(16)	58.3(2)	B(2)−B(1)−B(4)	109.4(3)	109.4(4)
B(2)−S(6)−B(7)	57.90(17)	57.73(18)	B(3)−B(1)−B(4)	59.9(2)	59.7(3)

(CO), 1437 m, 1095 m, 694 s, 541 m, 518 s, 487 m, 449 w, 417 w. LRMS (FAB $^+$): *m*/*z* 835 [M$^+$] (isotope envelope corresponding to the parent anion [Rh(phen)(PPh_3)(CO)]$^+$, 573 [M − PPh_3]$^+$, 545 [M − PPh_3 − CO]$^+$, 467 [M − PPh_3 − CO − Ph]$^+$, 390 [M − PPh_3 − CO −2Ph]$^+$, 283 [M − 2PPh_3 − CO]$^+$. ^{1}H NMR (300 MHz, $CDCl_3$, 300 K): 9.13 (d, 2H; $C_{12}H_8N_2$), 8.11 (d, 2H; $C_{12}H_8N_2$), 7.52 (m, 4H; $C_{12}H_8N_2$), 7.33 (m, 30H; PPh_3). ^{13}C NMR (300 MHz, CD_2Cl_2, 300 K): δ 193.20 (d, ^1J (^{103}Rh, ^{13}C) = 78 Hz, C−O), 151.44 (*o*-CH, $C_{12}H_8N_2$), 144.35 (*o*-C_{quart}, $C_{12}H_8N_2$), 137.68 (*p*-CH, $C_{12}H_8N_2$), 133.92 (CH, PPh_3), 133.34 (CH, PPh_3), 130.72 (C_{quart}, PPh_3), 128.31 (CH, PPh_3), 127.04 (*m*-CH, $C_{12}H_8N_2$), 124.64 (*m*-CH, $C_{12}H_8N_2$). ^{31}P NMR (121 MHz, $CDCl_3$, 233 K): 41.5 [d, ^1J(^{103}Rh−^{31}P) = 114 Hz, PPh_3]; ^{31}P NMR (121 MHz, $CDCl_3$, 300 K): 39.3 (br s, coupling not observed).

Results

A. [Rh(η^4-diene)(L_2)][SB_9H_{12}] Salts. 1. Preparation and Characterization. These salts were prepared by treatment of the rhodium complexes [RhCl(diene)]$_2$ [diene = cyclooctadiene (cod), norbornadiene (nbd)] with the N-heterocyclic ligands bpy, Me_2bpy, phen, and py in either ethanol or methanol at room temperature, followed by the addition of the thiaborane salt Cs[6-*arachno*-SB_9H_{12}], which resulted in the precipitation of the corresponding salts, **1**−**8** (Scheme 1).

The products were characterized by NMR spectroscopy, elemental analysis, and mass spectrometry. In addition, the structures of compounds **1** and **3** were determined by X-ray crystallographic analysis. The spectroscopic data were in accordance with values previously reported for [Rh(η^4-diene)(L_2)]$^+$ complexes partnered with inorganic anions such as PF_6^-, BF_4^-, or ClO_4^-.[17]

The ^{11}B NMR spectra of the eight salts contained six signals of 1:2:1:1:2:2 relative intensity between δ +3.4 and −37.0. The presence of the thiaborane anion was additionally confirmed in the ^{1}H NMR spectra, which featured a higher field resonance (ca. δ −1.80) that corresponds to the two BHB bridging hydrogen atoms, while the ^{1}H signals of the nine terminal and one *endo* BH hydrogens appeared in the positive region of the spectra between δ +3.00 and 0.00. These ^{11}B and ^{1}H NMR data match the values in the cesium salt, $CsSB_9H_{12}$, for which the full assignment of the NMR resonances has been reported.[18]

(17) (a) Brodzki, D.; Pannetier, G. *J. Organomet. Chem.* **1976**, *104*, 241−251. (b) Usón, R.; Oro, L. A.; Claver, C.; Garralda, M. A. *J. Organomet. Chem.* **1976**, *105*, 365−370. (c) Robertson, J.; Kadziola, A.; Krause, R. A.; Larsen, S. *Inorg. Chem.* **1989**, *28*, 2097−2102. (d) Dorta, R.; Shimon, L.; Milstein, D. *J. Organomet. Chem.* **2004**, *689*, 751−758. (e) Ribeiro, P. E. A.; Donnici, C. L.; dos Santos, E. N. *J. Organomet. Chem.* **2006**, *691*, 2037−2043.

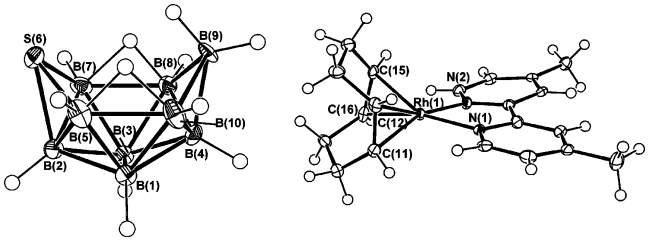

Figure 1. ORTEP-type diagrams depicting the molecular structures and label schemes of the $[SB_9H_{12}]^-$ anion and the $[Rh(cod)(Me_2bpy)]^+$ cation in **3**.

In agreement with the formulation of the salts, the ^1H NMR spectra also contained the resonances for the organometallic cations $[Rh(\eta^4\text{-diene})(L_2)]^+$. For the $[Rh(\eta^4\text{-cod})(L_2)]^+$ complexes in **1**, **3**, **5**, and **7**, the vinyllic and two allylic multiples appeared near δ 4.60, 2.65, and 2.24, respectively, whereas the nbd signals of the $[Rh(\eta^4\text{-nbd})(L_2)]^+$ complexes in **2**, **4**, **6**, and **8** were found close to δ 4.60 (vinyllic), 4.10 (2CH, nbd), and 1.55 (CH_2, nbd). The proton resonances of the coordinated N-donor ligands were found in the aromatic region of the spectra. In addition, the low-resolution mass spectra of the eight salts exhibited the molecular ions of the parent organometallic cations, $[Rh(\eta^4\text{-diene})(L_2)]^+$, and the daughter ions that result from the fragmentation of the diene ligands.

2. Structure of $[Rh(cod)(L_2)][SB_9H_{12}]$ [L_2 = bpy (1), Me_2bpy (3)]. A summary of the crystallographic data and selected bond distances and angles are given in Tables 1 and 2, respectively. The solid-state structures are in agreement with the NMR data, confirming that **1** and **3** are salts of the 16-electron square-planar cations, $[Rh(cod)(bpy)]^+$ and $[Rh(cod)(Me_2bpy)]^+$, respectively, and the 10-vertex *arachno*-thiaborane, $[6\text{-}SB_9H_{12}]^-$ anion (Figure 1). Although these ions have been crystallographically investigated in $CsSB_9H_{12}$, $[Au(PPh_3)][SB_9H_{12}]$, and $[Rh(cod)(bpy)][PF_6]$,[18−20] there are few structural studies of organometallic/thiaborane salts.[18] X-ray crystallographic studies of **1** and **3** were deemed appropriate to investigate possible interionic interactions between the *arachno*-thiaborane cluster and the square-planar d^8-Rh complex.

The thiaborane anion in **1** exhibited an occupancy disorder between S(6) and B(9), which was modeled including geometry restrains for both atoms and complementary occupancy factors. The dimensions of $[SB_9H_{12}]^-$ in **1** and **3** are comparable to those found for the thiaborane in $CsSB_9H_{12}$[18] and $[Rh(H)_2(bpy)(PPh_3)_2][SB_9H_{12}]$ (**19**; this work). In particular, the distances B(2)−B(5) and B(2)−B(7) flanking the sulfur atom are longer than the corresponding distances B(4)−B(8) and B(4)−B(10) (Table 2), and the apical boron atom of connectivity three B(9) is ca. 0.20 Å closer to B(4) than to B(8) and B(10). This interatomic length pattern is common to all the crystallographically determined 10-vertex [*arachno*-6-$SB_9H_{12}]^-$ clusters.[18,19]

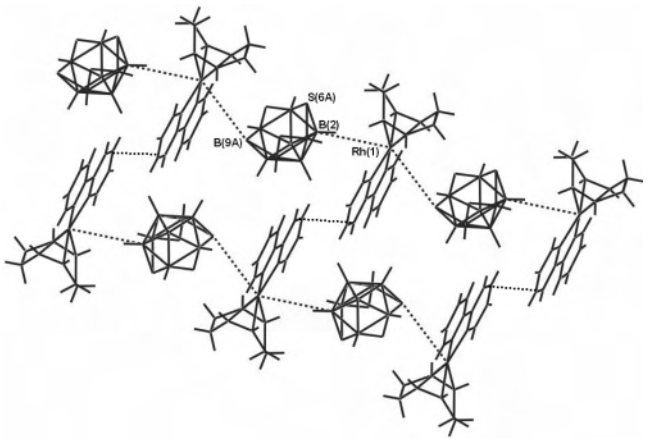

Figure 2. Packing illustration of **1**, showing short interionic contacts.

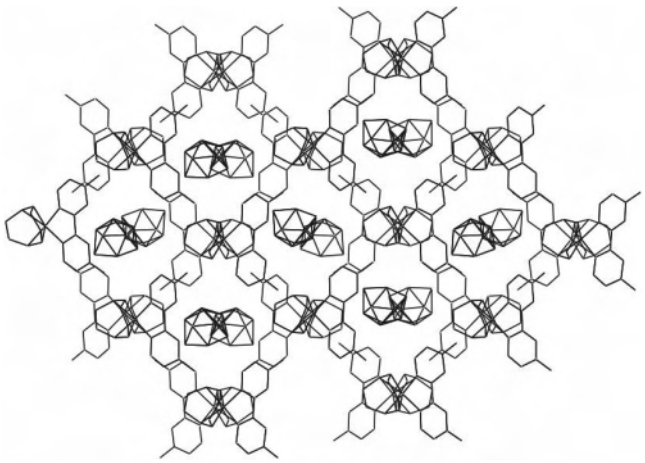

Figure 3. Packing of **3** viewed along the *c*-axis.

The crystal structure of **1** can be described as columns of $[Rh(\eta^4\text{-cod})(bpy)]^+$ and $[SB_9H_{12}]^-$ ions that stack in an alternate fashion along the *c*-axis (Figure 2). The closest Rh···B contacts are 3.8540(3) and 3.8882(2) Å for B(2) and B(9), respectively; within the columns, the $[Rh(cod)(bpy)]^+$ complexes adopt an eclipsed disposition, leading to short distances [the shortest for C(8)···C(9) at 3.4828(3) Å] between the bipyridine ligands of adjacent parallel chains (Figure 2). These $A^-\cdots C^+$ chains stack parallel to the *ac* plane, forming layers that pack along the *b* direction.

In the crystal structure of **3**, there are two crystallographically independent anions and cations/unit cell. Similarly to **1**, the crystal structure of **3** may be viewed as ribbons of $[Rh(cod)(Me_2bpy)]^+$ and $[SB_9H_{12}]^-$ that stack in an alternating manner along the crystallographic *b*-axis. In contrast, however, there is only one short interionic Rh···B distance/independent rhodium complex at 4.005(5) and 4.062(5) Å, which corresponds to thiaborane anions that stack above the square-planar metal complexes.

In a different view, the structure of **3** can be described as channels of $[Rh(cod)(Me_2bpy)]^+$ cations filled with $[SB_9H_{12}]^-$ anions along the *c*-axis (Figure 3). In the channels, the anions are close to the chelating ligands, cod and Me_2bpy, with an average B···C distance of ca. 4.00 Å.

The Rh···B distances in **1** and **3** are far from the bonding Rh−B lengths at 2.391(3) and 2.385(3) Å that were found

(18) Nestor, K.; Fontaine, X. L. R.; Greenwood, N. N.; Kennedy, J. D.; Thornton-Pett, M. *J. Chem. Soc., Dalton Trans.* **1991**, 2657−2667.
(19) Guggenberger, L. J. *J. Organomet. Chem.* **1974**, *81*, 271.
(20) Felix, A.; Guadalupe, A. R.; Huang, S. D. *Z. Kristallogr.-New Cryst. Struct.* **1999**, *214*, 463.

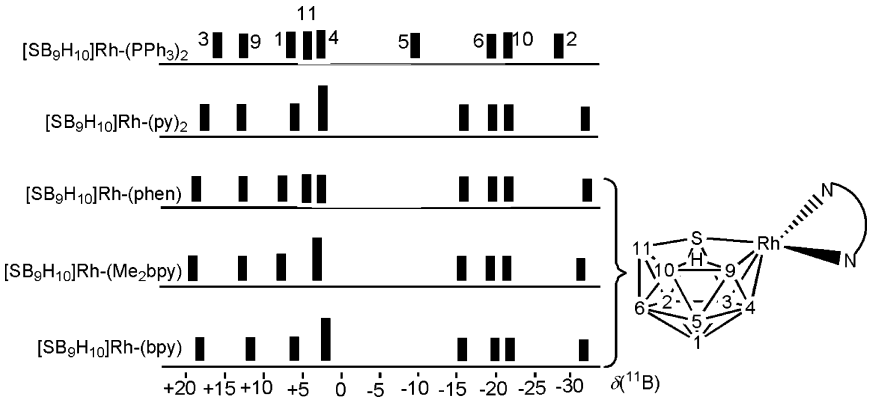

Figure 4. Stick representation of the ^{11}B NMR resonances for [8,8-(L_2)-8,7-$RhSB_9H_{10}$].

in [Rh(cod)($HCB_{11}H_{11}$)],[21] where the {Rh(η^4-cod)} fragment is linked to the carborane ligand through *exo*-polyhedral Rh−H−B bonds; alternatively, the Rh···B distances in the new reagents, **1** and **3**, are similar to the closest B···Rh contact at ca. 4.1 Å in the related [Rh(η^4-cod)($THF)_2$][($HCB_{11}H_{11}$)] salt,[21a] which also exhibits a columnar anion/cation packing with the monocarborane anions occupying two opposite positions in the resulting pseudooctahedral environment of the rhodium(I) element.

B. Synthesis and Characterization of New Rhodathiaboranes. 1. [8,8-(L_2)-*nido*-8,7-$RhSB_9H_{10}$]. Solutions of the nbd−Rh salts [Rh(η^4-nbd)(L_2)][SB_9H_{12}] [L_2 = bpy (**2**), Me_2-bpy (**4**), and phen (**6**)] in dichloromethane at room temperature evolved into the corresponding 11-vertex *nido*-rhodathiaboranes of general formula [8,8-(L_2)-*nido*-8,7-$RhSB_9H_{10}$] [L_2 = bpy (**9**), Me_2bpy (**10**), phen (**11**)]. The conversion rates of the nbd−Rh(I) salts decreased in the sequence **6** > **2** > **4**, with half-lifes of 2, 4, and 7 h, respectively. Similarly, the pyridyl−Rh salts [Rh(η^4-diene)-($py)_2$][SB_9H_{12}] [diene = cod (**7**), nbd (**8**)] afforded the analogous rhodathiaborane [8,8-($py)_2$-*nido*-8,7-$RhSB_9H_{10}$] (**12**), but the reactions took place in minutes either at room or low temperature.

In contrast, [Rh(η^4-cod)(bpy)]$^+$ and [Rh(η^4-cod)(Me_2-bpy)]$^+$ gave mixtures of the rhodathiaboranes **9** and **10** and new uncharacterized species, whereas the cod−Rh(I) starting material, **5**, afforded selectively a new polyhedral boron-containing compound. This compound has not been fully characterized, but the NMR data, included in deposited material for this article, showed that it is fluxional, in a process that appears to involve the 10-vertex boat-type {SB_9H_{11}}-cluster and a {Rh(cod)(phen)}-fragment. The resemblance of the ^{11}B NMR spectrum to that of the starting [SB_9H_{12}]$^-$ anion suggests that the {Rh(cod)(phen)}-fragment could be bound to the polyhedral cluster through Rh−H−B bonds, which would resemble the binding in fully characterized *exo*-polyhedral carboranes.[21] In any event, these results demonstrate the different reactivity of the cod−Rh reagents, **1**, **3**, and **5**, compared with the nbd−Rh counterparts, **2**, **4**, and **6**.

The 11-vertex *nido*-rhodathiaborane **12** is very unstable, and it was only characterized in situ by NMR spectroscopy. Although more stable than the pyridine-ligated derivative **12**, the 11-vertex L_2−Rh *nido*-analogues **9**−**11** also decompose after several days in solution. However, they were sufficiently stable to allow their characterization by NMR spectroscopy and mass spectrometry.

The ^{11}B NMR spectra of all these 11-vertex *nido*-metallathiaboranes contained nine resonances from δ 20.0 to −32.0; in all the spectra, there was a group of five resonances in the positive region and a set of four signals in the negative area. The average separation between these higher field and lower field groupings is 18 ppm. The phosphine-ligated rhodathiaborane [8,8-($PPh_3)_2$-*nido*-7,8-$RhSB_9H_{10}$][10] exhibits the same grouping of lower field ^{11}B-resonances; in contrast, the gap with the other four higher field signals is smaller than that found for **9**−**12** (Figure 4).

2. [8,8-(L_2)-8-(L')-*nido*-8,7-$RhSB_9H_{10}$]. The rhodathiaboranes of general formula [8,8-(L_2)-8-PPh_3-*nido*-8,7-$RhSB_9H_{10}$] [L_2 = bpy (**13**), Me_2bpy (**14**), phen (**15**)] can be prepared by either (i) treatment of the diene−Rh salts **1**−**4** or **6** with PPh_3 in methanol or ethanol at room temperature under a hydrogen atmosphere or (ii) by reaction in CH_2Cl_2 of the nbd−Rh cations [Rh(η^4-nbd)(L_2)]$^+$ in the presence of PPh_3. However, under the same conditions with H_2(g), the phen-containing reagent, **5**, did not afford the 11-vertex *nido*-rhodathiaborane **15** but the salt [Rh($H)_2$(phen)($PPh_3)_2$]-[SB_9H_{12}] (see below).

The acetonitrile-ligated analogues [8,8-(L_2)-8-($NCCH_3$)-*nido*-8,7-$RhSB_9H_{10}$] [L_2 = bpy (**16**), Me_2bpy (**17**), phen (**18**)] were formed upon dissolution of the L_2-ligated *nido*-rhodathiaboranes **9**−**11** in CH_3CN. Alternatively, they can be prepared from the nbd−Rh salts **2**, **4**, and **6** and an excess of CH_3CN in CH_2Cl_2 solution. Both series of phosphine- and acetonitrile-bearing metallathiaboranes are the result of addition of the Lewis bases, PPh_3 or CH_3CN, to the formally unsaturated rhodium center of the L_2−Rh *nido*-compounds, **9**−**11**, affording clusters with the same *nido*-geometry but one additional skeletal electron pair.

(21) (a) Weller, A. S.; Mahon, M. F.; Steed, J. W. *J. Organomet. Chem.* **2000**, *614*, 113−119. (b) Knobler, C. B.; Marder, T. B.; Mizusawa, E. A.; Teller, R. G.; Long, J. A.; Behnken, P. E.; Hawthorne, M. F. *J. Am. Chem. Soc.* **1984**, *106*, 2990. (c) Long, J. A.; Marder, T. B.; Behnken, P. E.; Hawthorne, M. F. *J. Am. Chem. Soc.* **1984**, *106*, 2979.

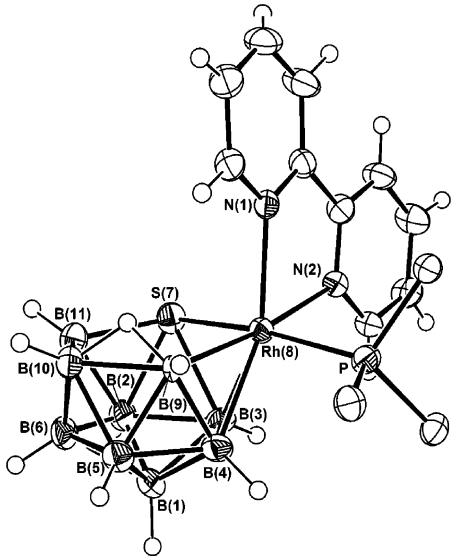

Figure 5. Molecular structure and labeling scheme of **13**.

Table 3. Selected Interatomic Lengths (Å) and Angles (deg) for [8,8-(bpy)-8-(PPh_3)-*nido*-$RhSB_9H_{10}$] (**13**)

Rh(8)−N(1)	2.178(3)	Rh(8)−B(9)	2.197(5)
Rh(8)−N(2)	2.208(3)	S(7)−B(11)	1.913(6)
Rh(8)−P	2.3210(16)	B(6)−B(11)(shortest)	1.719(8)
Rh(8)−S(7)	2.3592(16)	S(7)−B(2)	1.969(6)
Rh(8)−B(3)	2.171(6)	S(7)−B(3)	2.073(5)
Rh(8)−B(4)	2.196(6)	B(2)−B(3)(longest)	1.913(8)
B−B(av)	1.899(8)		
N(1)−Rh(8)−N(2)	74.64(12)	S(7)−Rh(8)−B(9)	89.60(12)
S(7)−Rh(8)−P	170.30(5)	N(1)−Rh(8)−P	93.46(9)
N(2)−Rh(8)−P	90.91(10)	N(2)−Rh(8)−B(9)	173.00(15)
N(1)−Rh(8)−B(3)	147.75(15)	N(1)−Rh(8)−B(4)	149.81(18)
B(3)−Rh(8)−B(4)	49.0(2)	B(2)−S(7)−B(3)	56.4(2)

Compounds **13**−**15** were characterized by NMR spectroscopy and mass spectrometry. In addition, **14** and **15** were also characterized by elemental analysis, and the structure of the bipyridine derivative, **13**, was determined by X-ray diffraction analysis. This rhodathiaboreane consists of an 11-vertex polyhedron notionally derived from a *closo*-icosahedron by removal of a vertex. The pentagonal open face of the new rhodathiaborane is formed by the {Rh(bpy)(PPh_3)} fragment, a sulfur atom, and three BH units, with a BHB bridging hydrogen atom at the B(9)−B(10) edge (Figure 5). Distances and angles are given in Table 3 and fall within the ranges of existing structural data on related rhodathiaboranes.[10,11]

In **13**, the bipyridine ligand chelates the rhodium center at positions that are trans to B(9) and the B(3)−B(4) edge with the PPh_3 group trans to the sulfur atom S(7). The rhodium center could be described as 5-coordinate and may be formally regarded as an 18-electron complex between the $\{Rh(PPh_3)(bpy)\}^+$ unit and an $\{SB_9H_{10}\}^-$ anionic fragment that acts as a bidentate ligand in an η^4-fashion. Alternatively, within the general electron-counting and cluster-geometry approach to polyhedral boron compounds,[22] this rhodathiaborane is a 26-electron system for which the observed 11-vertex *nido*-structure is predicted.

(22) (a) Wade, K. *Adv. Inorg. Chem. Radiochem.* **1976**, *18*, 1−66. (b) Williams, R. E. *Adv. Inorg. Chem. Radiochem.* **1976**, *18*, 67−142.

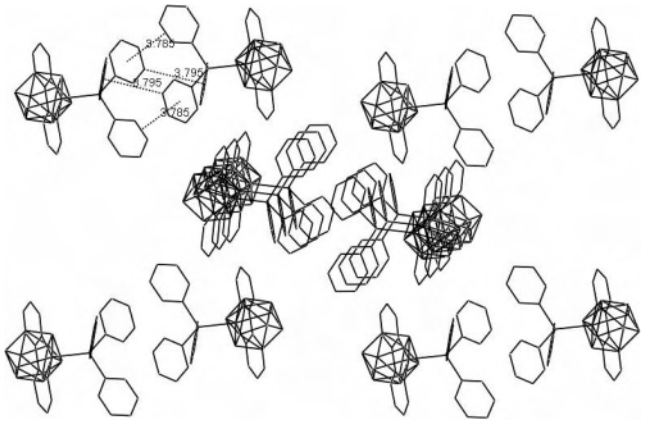

Figure 6. Packing diagram of the crystal structure of **13** along the *a*-axis.

There are three ideal configurations of the metal coordination environment for {Rh(bpy)(PPh_3)} fragment with respect to the {S(7)B(3)B(4)B(9)} face, and compound **13** exhibits that shown in schematic **A**. This ligand configuration was also found in [8,8-(η^2-dppe)-8-(CO)-*nido*-8,7-$RhSB_9H_{10}$] (dppe = $Ph_2PCH_2CH_2PPh_2$).[23] By contrast, the dangling unidentate dppm-ligand in the isoelectronic 11-vertex rhodathiaborane [8,8-(η^2-dppm)-8-(η^1-dppm)-*nido*-8,7-$RhSB_9H_{10}$] is *trans* to the B(3)−B(4) edge, configuration **B**,[11d] and the acetonitrile derivative [8,8-(η^2-dppe)-8-($NCCH_3$)-*nido*-8,7-$RhSB_9H_{10}$][23] exhibits the configuration **C**, in which the $NCCH_3$ ligand is trans to B(9).

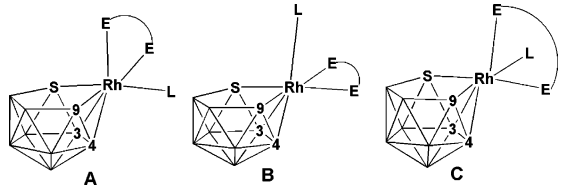

In the crystal structure of **13**, the rhodathiaborane clusters associate in pairs through sextuple phenyl embrace (SPE) interactions (Figure 6). The P···P separation and the Rh−P···P−Rh colinearity are 6.9 Å and 172°, respectively, and fall in the range reported for this attractive edge-to-face interaction.[24] The resulting rhodathiaborane "dimers" pack along the *a*-axis, forming ribbons in which the bipyridine ligands face the thiaborane cages of adjacent clusters at short B···C contacts, the shortest being 3.7 Å (Figure 6).

The NMR spectra of **13** agree with the molecular structure found in the solid state. A comparison with the NMR data of **14**−**18** permitted the characterization of all the compounds as 11-vertex *nido*-rhodathiaboranes that incorporate a {Rh(L_2)(L′)}-moiety into the cluster framework (L_2 = bpy, Me_2-bpy, phen; L′ = PPh_3, $NCCH_3$). The ^{11}B NMR spectra of the PPh_3-ligated derivatives were broader than those of the $NCCH_3$-ligated analogues, reflecting the larger bulkiness of the former compounds. There were five boron resonances that group at lower fields than the other four-boron signals; the gap between these groupings was, however, smaller than

(23) Adams, K. J.; McGrath, T. D.; Rosair, G. M.; Weller, A. S.; Welch, A. J. *J. Organomet. Chem.* **1998**, *550*, 315−329.
(24) Dance, I.; Scudder, M. *J. Chem. Soc., Chem. Commun.* **1995**, 1039−1040.

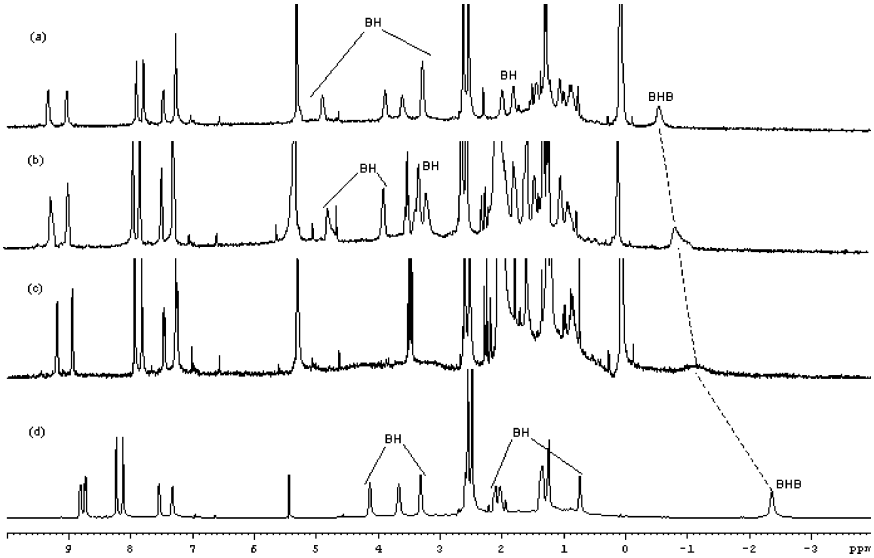

Figure 7. ^{1}H{^{11}B} spectra of [8,8-(Me$_2$bpy)-*nido*-8,7-RhSB$_9$H$_{10}$] (**10**): (a) in $CDCl_3$; (b) in $CDCl_3$ with a 1 to 4 ratio of **10** to CH_3CN; (c) in $CDCl_3$ with a 1 to 20 ratio of **10** to CH_3CN; (d) in CD_3CN.

in **9**−**12**. In addition, the average chemical shift of the boron resonances of the L′-adducts (L′ = PPh_3, $NCCH_3$), **13**−**18**, shifted slightly toward higher fields with respect to **9**−**12**.

The ^{31}P NMR spectra of the PPh_3-ligated adducts, **13**−**15**, contained a sharp doublet at room temperature that confirms the presence of the PPh_3−Rh linkage. In contrast, the $NCCH_3$ ligand in **16**−**18** dissociates in $CDCl_3$ solutions to give **9**−**11**. In CD_3CN solvent, however, the ^{1}H{^{11}B} NMR signal of the BHB bridging hydrogen atom shifts considerably to high field with respect the same resonance in chloroform (see Figure 7). As described below, we have found that a high-field shift of the BHB-bridging resonance is a good diagnostic of Rh−L′ binding in 11-vertex *nido*-rhodathiaboranes that incorporate 16-electron {Rh(L$_2$)}-fragments. Moreover, addition of excess of acetonitrile to solutions of the *nido*-rhodathiaboranes **9**−**11** in $CDCl_3$ results (i) in a shift of the ^{1}H NMR cluster resonances toward lower frequencies and (ii) in a broadening of the signals (Figure 7). These results are consistent with fast exchange between Rh-coordinated and free acetonitrile:

$$[8,8\text{-}(L_2)\text{-}8,7\text{-}RhSB_9H_{10}] + CH_3CN \rightleftharpoons [8,8\text{-}(L_2)\text{-}8\text{-}(NCCH_3)\text{-}8,7\text{-}RhSB_9H_{10}] \quad (1)$$

A comparison between the BHB-proton resonance positions in the series of compounds reported here and previously reported 11-vertex *nido*-rhodathiaboranes reveals that this signal shifts significantly depending on the nature and the number of the Rh-bound *exo*-polyhedral ligands (Figure 8). Thus, there is a move toward lower field on replacing the PPh_3 ligand in [8,8-(PPh_3)$_2$-*nido*-8,7-RhSB$_9$H$_{10}$] by either pyridine or bipyridine in **12** and **9**. By contrast, in the analogue [8,8-(η^2-dppe)-*nido*-8,7-RhSB$_9$H$_{10}$],[23] the BHB resonance shifts toward higher field. It is also evident that saturation of the rhodium center by PPh_3 and η^1-dppm in **13** and [8,8-(η^2-dppm)-8-(η^1-dppm)-8,7-RhSB$_9$H$_{10}$],[11d] respectively, results in a shift to higher field with respect to the unsaturated rhodathiaboranes **9** and [8,8-(η^2-dppe)-8,7-RhSB$_9$H$_{10}$].[23] This suggests that the higher field shift of the BHB proton resonance correlates with a negative charge buildup on the metal center of the 11-vertex rhodathiaboranes [PPh_3 vs dppe; (L$_2$)−Rh vs (L$_2$)(L′)−Rh]. According to this charge/BHB proton-shift relationship, the superior σ-donor character of the bpy ligand relative to the PPh_3 groups would entail a higher negative charge on the rhodium center and a consequent shift of the BHB proton resonance to higher fields. On this rationale, it is, therefore, contradictory that the BHB bridging hydrogen signal in **9** appears at lower fields than in the PPh_3 derivative, [8,8-(PPh_3)$_2$-*nido*-8,7-RhSB$_9$H$_{10}$]. A similar π-acceptor character of the N-heterocyclic ligands relative to the phosphine ligands[25] could imply a higher degree of charge delocalization over the cluster in the L$_2$-ligated rhodathiaboranes (L$_2$ = py, bpy, Me$_2$-bpy, phen), which would result in a marked different trans-effect to the BHB hydrogen atom.

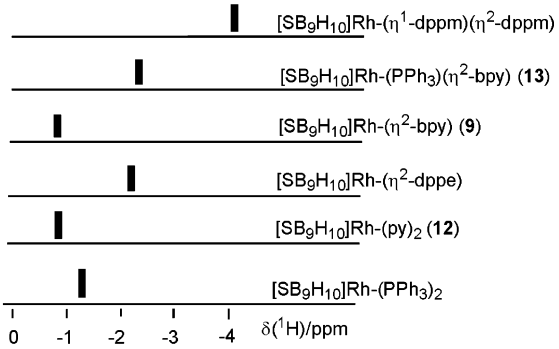

Figure 8. Stick representation of the B(9)−H−B(10) bridging proton resonance for [8,8-(L$_2$)-*nido*-8,7-RhSB$_9$H$_{10}$] and [8,8-(L$_2$)-8-(L)-*nido*-8,7-RhSB$_9$H$_{10}$].

C. Synthesis and Characterization of Other Salts. 1. [Rh(H)$_2$(L$_2$)(PPh$_3$)$_2$][SB$_9$H$_{12}$] (L$_2$ = bpy, Me$_2$bpy, phen). The treatment of **1**−**4** and **6** with an excess of PPh_3 in an H_2(g) atmosphere yielded, as described above, the corre-

(25) Leyssens, T.; Peeters, D; Orpen, A. G.; Harvey, J. N. *Organometallics* **2007**, *26*, 2637.

sponding 11-vertex rhodathiaboranes, **13**−**15**. By using stoichiometric amounts of PPh_3 in an H_2(g) atmosphere, the starting salts afforded mixtures that contained the corresponding 11-vertex {$Rh(L_2)(PPh_3)$}−*nido*-rhodathiaboranes, the starting [$Rh(\eta^4$-diene)$(L_2)]^+$ complexes, and the d^6-rhodium dihydrides, $[Rh(H)_2(L_2)(PPh_3)_2]^+$ (L_2 = bpy, Me_2bpy, phen), in different proportions. In contrast, [Rh(cod)(phen)][SB_9H_{12}] (**5**), under the same conditions, afforded selectively the [$Rh(phen)(PPh_3)_2(H)_2$][SB_9H_{12}] salt, with either excess or stoichiometric amounts of phosphine.

On the other hand, the treatment of the pyridine-containing salts **7** and **8** with PPh_3 in H_2(g) atmosphere afforded [8,8-$(PPh_3)_2$-*nido*-8,7-$RhSB_9H_{10}$],[10] which is most likely the result of {$Rh(py)_2$}-fragment insertion/py substitution reactions.

In view of these results, we used an indirect route for the synthesis and isolation of new $[Rh(H)_2(L_2)(PPh_3)_2][SB_9H_{12}]$ [L_2 = bpy (**19**), Me_2bpy (**20**), phen (**21**)] salts, which consisted of the treatment of the dimers $[RhCl(\eta^4$-diene$)]_2$ (diene = cod, nbd) with PPh_3 in the presence of H_2(g), followed by addition of $CsSB_9H_{12}$ to precipitate the Rh−hydride/thiaborane salts in either methanol or ethanol.

The ^{11}B spectra of **19**−**21** in $CDCl_3$ exhibited the signals of the thiaborane anion $[SB_9H_{12}]^-$ as the only boron-containing species, and the $^1H\{^{11}B\}$ NMR spectra confirmed the partnership of this anion with the corresponding d^6-rhodium cations, $[Rh(H)_2(L_2)(PPh_3)_2]^+$. The proton resonances of the N-donor and triphenylphosphine ligands displayed the expected relative intensities when compared with the proton resonances of the thiaborane cluster. In addition, there was an apparent quartet close to δ −15.50, which became a doublet in the $^1H\{^{31}P\}$ spectra of the salts and corresponds to the hydride ligands. In turn, the $^{31}P\{^1H\}$ NMR spectrum contained a doublet, which through the series is close to δ +47.0.

The $[Rh(H)_2(bpy)(PPh_3)_2]^+$ complex **19** was first isolated with typical inorganic anions (BF_4^-, ClO_4^-, PF_6^-, etc.);[26] however, neither their NMR data were reported nor were their crystallographic structures determined. Thus, we carried out a crystallographic study of **19**, aimed at measuring structural parameters of the Rh(III) complex and analyzing potential interionic interactions.

The molecular structure of the cationic d^6-Rh(III) complex in the salt **19** is depicted in Figure 9, and some selected distances and angles are gathered in Table 4. The quality of the crystal allowed the location of all the hydrogen atoms of the thiaborane anion: nine BH terminal, two BHB bridging, and one *endo*-B(9)−H. The molecular dimensions of the cluster are similar to those found in **1** and **3**, and they are commented upon above.

The cation $[Rh(H)_2(bpy)(PPh_3)_2]^+$ exhibits a distorted octahedral coordination sphere around the rhodium(III) atom. In agreement with the NMR data, the two phosphine groups are trans to each other, and the hydrides occupy positions trans to the nitrogen atoms of the chelating bpy ligand. The bond distances are within the range found in reported

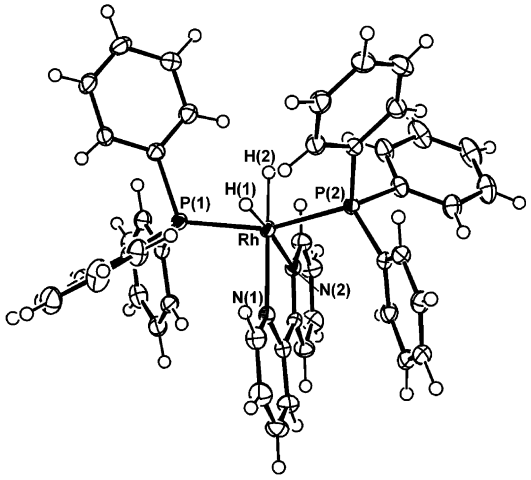

Figure 9. ORTEP-type illustration of $[Rh(H)_2(bpy)(PPh_3)_2]^+$ in **19**.

Table 4. Selected Interatomic Lengths (Å) and Angles (deg) for $[Rh(H)_2(bpy)(PPh_3)_2][SB_9H_{12}]$ (**19**)

Rh(1)−P(1)	2.2941(9)	Rh(1)−N(1)	2.164(3)
Rh(1)−P(2)	2.3004(9)	Rh(1)−N(2)	2.146(3)
S(6)−B(2)	1.954(5)	S(6)−B(5)	1.949(5)
S(6)−B(7)	1.946(5)	B(2)−B(5)	1.905(6)
B(2)−B(7)	1.888(7)	B(4)−B(8)(shortest)	1.728(6)
B(9)−B(4)	1.738(6)	B(9)−B(8)(longest)	1.918(6)
B(9)−B(10)	1.910(6)		
P(1)−Rh(1)−P(2)	159.75(3)	N(1)−Rh(1)−N(2)	76.06(10)
P(1)−Rh(1)−N(1)	99.42(8)	B(2)−S(6)−B(7)	57.9(2)
P(1)−Rh(1)−N(2)	98.43(8)	B(2)−S(6)−B(5)	58.43(18)
P(2)−Rh(1)−N(1)	97.25(8)	B(2)−B(1)−B(3)	58.8(3)
P(2)−Rh(1)−N(2)	96.69(8)	B(2)-B(1)-B(4)	109.1(3)

rhodium(III) *cis*-dihydrido complexes with N-chelating ligands.[27] A structural feature of **19** and related hexacoordinated rhodium(III) complexes[27] is the bending of the phosphine ligands toward the hydrides resulting in P−Rh−P bond angles close to 160°.

In the extended crystal structure of **19**, each $[Rh(H)_2(bpy)(PPh_3)_2]^+$ cation exhibits two SPE interactions that lead to the formation of chains along the P−Rh−P direction. In addition, as shown in Figure 10, the bipyridine ligands on one chain penetrate the phenyl ring region of adjacent parallel chains. The result is the formation of zigzag layers of cations that grow parallel to the (101) crystallographic direction. The SB_9H_{12} anions pack between the layers in close proximity to the bpy ligands.

2. $[Rh(CO)(L_2)(PPh_3)_2][SB_9H_{12}]$ (L_2 = bpy, Me_2bpy, phen). Treatment of **1**−**6** with excess of triphenylphosphine in an atmosphere of carbon monoxide led to the formation of $[Rh(CO)(L_2)(PPh_3)_2][SB_9H_{12}]$ [L_2 = bpy (**22**), Me_2bpy (**23**), phen (**24**)], which were characterized by multinuclear NMR spectroscopy. The $^{31}P\{^1H\}$ NMR spectra of these species at low temperatures contained a doublet near δ +40.0, which broadened, became asymmetric, and eventually

(26) Cocevar, C.; Camus, A.; Mestroni, G. *J. Organomet. Chem.* **1972**, *35*, 389.

(27) (a) Ghedini, M.; Neve, F.; Lanfredi, A. M. M.; Ugozzoli, F. *Inorg. Chim. Acta* **1988**, *147*, 243−250. (b) Iglesias, M.; Del Pino, C.; Garciá-Blanco, S.; Martínez Carrera, S. *J. Organomet. Chem.* **1986**, *317*, 363−372. (c) Iglesias, M.; del Pino, C.; Nieto, J. L.; Garcia Blanco, S.; Martínez Carrera, S. *Inorg. Chim. Acta* **1988**, *145*, 91−98. (d) Iglesias, M.; del Pino, C.; San Jose, A.; Martínez-Carrera, S.; Ros, J. *J. Organomet. Chem.* **1989**, *366*, 391−401.

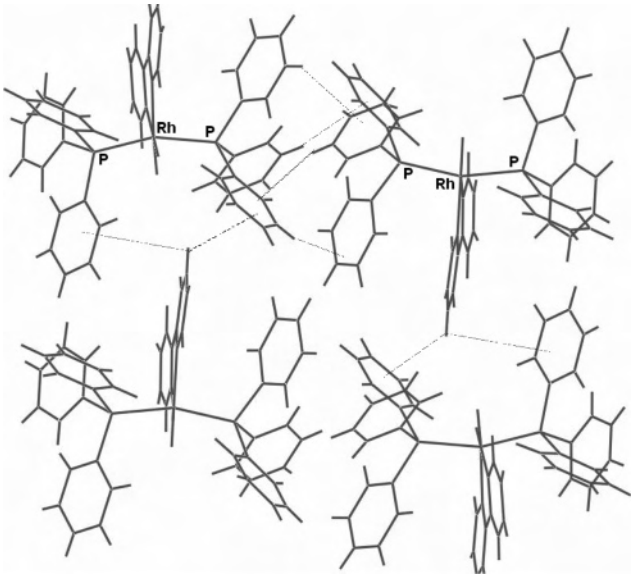

Figure 10. Illustration of SPE interactions in **19**.

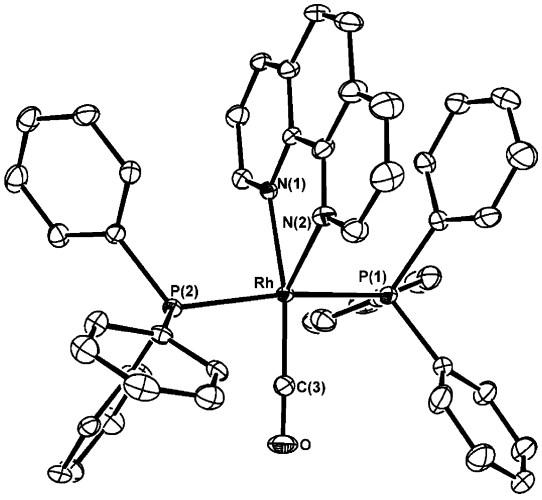

Figure 11. Molecular structure of [Rh(CO)(phen)(PPh$_3$)$_2$]$^+$ in **24**.

coalesced as the temperature was increased. Thus, at room and higher temperatures the $^1J(^{103}\text{Rh},^{31}\text{P})$ coupling constant was not observed.

This behavior was studied at different concentrations of free PPh_3 for the phen-derivative, **24**, and the data were analyzed by means of conventional line-shape programs. The values of *k* were found to be independent of the concentration of phosphine, indicating that they correspond to rates of PPh_3 dissociation from the five-coordinate cations. The activation parameters obtained form the Eyring plot, $\Delta H^{\ddagger} = 14 \pm 0.5$ kcal mol^{-1} and $\Delta S^{\ddagger} = 1 \pm 1$ eu, are consistent with a dissociative process.

The solid-state structure of **24** revealed the cation as an 18-electron rhodium(I) complex with a trigonal-bipyramidal geometry (Figure 11). The phosphine ligands lie trans to one another in the axial positions, while the phenanthroline and carbonyl occupy the equatorial positions. The Rh−N bond distances fall within the reported range 1.76−2.89 Å (Table 5); thus, the values are toward the longer end of the interval, which between 2.20 Å and the upper end point represents 11% of the reported Rh−N distances.

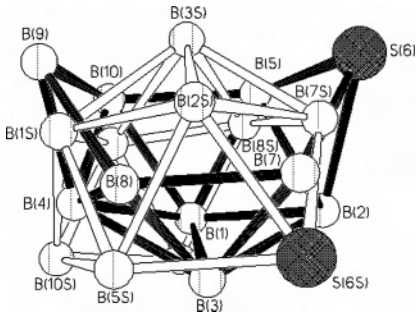

Figure 12. Model used for disordered thiaborane anions in **24**.

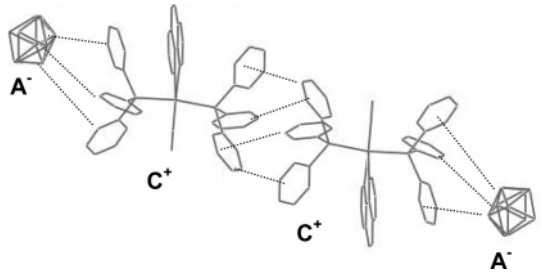

Figure 13. Illustration of SPE-driven intermolecular A$^-$···C$^+$···C$^+$···A$^-$ associations.

Table 5. Selected Bond Distances (Å) and Angles (deg) for [Rh(phen)(PPh$_3$)$_2$(CO)$_2$][SB$_9$H$_{12}$] (**24**)

Rh(1)−P(1)	2.3251(9)	Rh(1)−N(1)	2.355(3)
Rh(1)−P(2)	2.3168(9)	Rh(1)−N(2)	2.201(3)
Rh(1)−C(3)	1.793(3)	C(3)−O	1.154(4)
Rh(1)−C(3)−O	178.6(3)	P(1)−Rh(1)−C(3)	88.35(10)
P(1)−Rh(1)−P(2)	168.68(3)	N(2)−Rh(1)−P(2)	94.05(7)
P(2)−Rh(1)−C(3)	84.03(10)	N(1)−Rh(1)−C(3)	132.00(12)
N(1)−Rh(1)−P(1)	92.68(7)	N(2)−Rh(1)−C(3)	155.79(12)
N(2)−Rh(1)−P(1)	89.47(7)	N(1)−Rh(1)−N(2)	72.19(10)
N(1)−Rh(1)−P(2)	98.64(7)		

Likewise for the six-coordinate rhodium(III) dihydride complex in **19**, and related species,[27] the PPh_3 ligands of the five-coordinate cation in **24** bend toward the carbonyl ligand, forming an angle of 168.68(3)° that is 9° larger than the corresponding P−Rh−P angle in [Rh(H)$_2$(phen)(PPh$_3$)]$^+$.

The thiaborane anion was found to be disordered, and the molecular parameters are not discussed. It was modeled as two interwoven molecules as illustrated in Figure 12. In the crystal structure of **24**, the metal complexes exhibit SPE interactions that lead to intercationic "dimers" that are intercalated between two thiaborane anions. The result is the formation of A$^-$···C$^+$···C$^+$···A$^-$ associations that pack along the *a* direction (Figure 13).

Discussion

Scheme 2 illustrates that the main result of the reactivity of the square-planar Rh(I)/thiaborane saltlike compounds is formation of 11-vertex *nido*-rhodathiaboranes. These reagents exhibit significant differences in reaction rates, selectivities, and products that depend on the composition of the metal complexes. Thus, the [Rh(nbd)(L$_2$)]$^+$ cations, containing N-chelating ligands, react faster with the polyhedral thiaborane, [SB$_9$H$_{12}$]$^-$, than the cod−Rh congeners, [Rh(cod)(L$_2$)]$^+$, either in the presence or the absence of molecular hydrogen. More importantly, the nbd−Rh salts **2**, **4**, and **6** afford the

Scheme 2

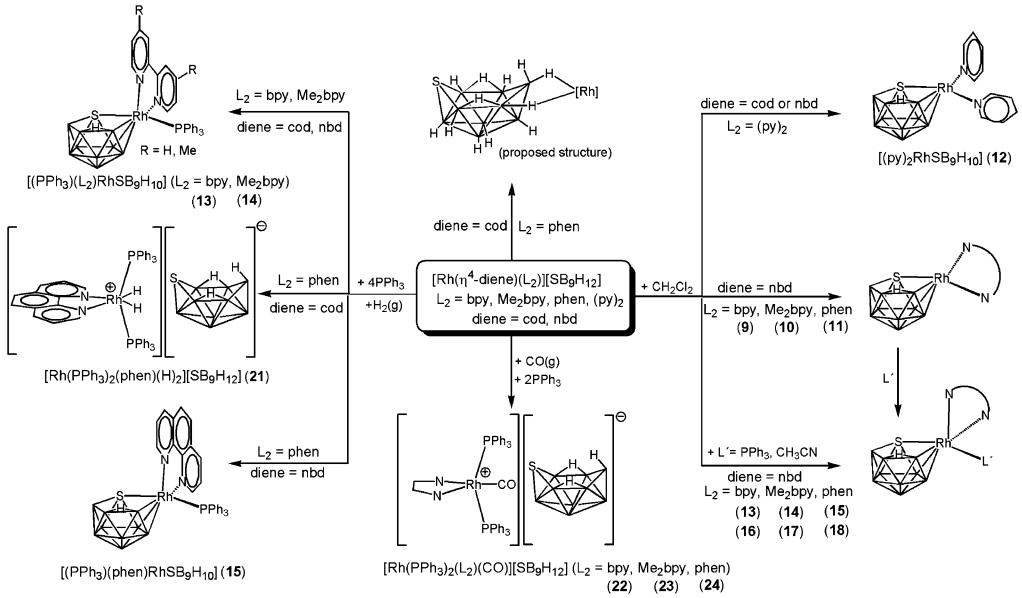

Scheme 3

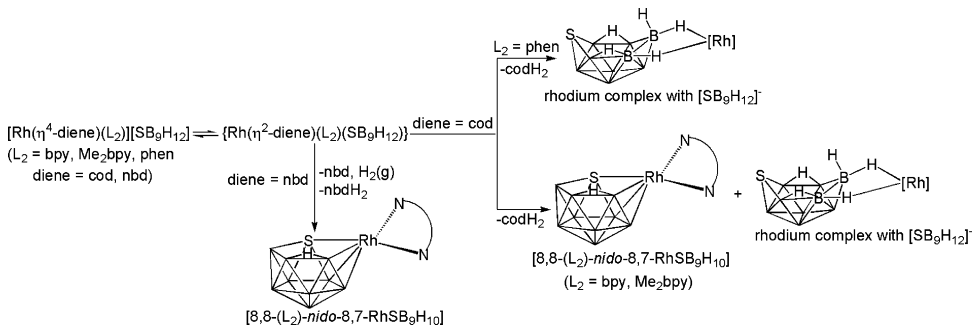

corresponding rhodathiaboranes **9**−**11** as the only polyhedral boron-containing compounds whereas the cod−Rh reagents **1**, **3**, and **5** yield mixtures of 11-vertex *nido*-rhodathiaboranes and a new (not fully characterized) species. We propose that these new compounds are *exo*-polyhedral Rh complexes with the thiaborane cluster $[SB_9H_{12}]^-$ acting as a ligand through its hydridic BH bonds. The nbd−Rh reagents lead to higher reaction rates and selectivities in the synthesis of new *nido*-rhodathiboranes that contain the Rh-bound N-chelating ligands bpy, Me_2bpy, and phen.

Within each diene−Rh class, the N-heterocyclic ligands further determine the insertion reaction rates, which for the nbd−Rh reagents decrease in the sequence **6** (phen) > **2** (bpy) > **4** (Me_2bpy). The same order is observed for the transformation of the cod−Rh salts, **1**, **3**, and **5**, which react much more slowly than the nbd analogues. In contrast to the N-chelators, the pyridine ligands in **7** and **8** enhance dramatically the reactivity of the Rh(I) square-planar cations $[Rh(\eta^4\text{-diene})(py)_2]^+$ with the polyhedral thioborane anion $[SB_9H_{12}]^-$, leading to instantaneous formation of the 11-vertex *nido*-rhodathiaborane **12**. Thus, the pyridine ligand determines the reactivity of the salts.

The formation of the new 11-vertex rhodathiaboranes **9**−**12** implies the insertion of a $\{Rh(L_2)\}$-fragment [L_2= bpy, Me_2bpy, phen, $(py)_2$] into the $\{SB_9H_{10}\}$-cage with concomitant elimination of the η^4-diolefin ligands from the metal complex and two hydrogen atoms from the thiaborane cluster. In the absence of hydrogen, we have found (by NMR and GC-MS) that the final mixtures resulting from the reactions of the nbd−Rh(I) cations with the $[SB_9H_{12}]^-$ anions in **2**, **4**, and **6** contain the diolefin nbd and its reduction product norbornene ($nbdH_2$) whereas, under the same conditions, the cod−Rh(I) reagents afford only the partially hydrogenated product cyclooctene ($codH_2$). These general observations suggest that the reactions between the square-planar Rh(I) cations and the thiaborane anion may proceed through two main pathways: (a) partial substitution of the η^4-diolefin ligand by the thiaborane cluster to give incipient $[Rh(\eta^2\text{-diene})(L_2)(SB_9H_{12})]$ complexes that can subsequently undergo elimination of the η^2-coordinated diolefin and molecular hydrogen, thus leading to the final insertion of the $\{Rh(L_2)\}$-fragment [L_2 = bpy, Me_2bpy, $(py)_2$]; (b) transfer of two hydrogen atoms from the thiaborane cluster to the η^4-diene ligand, forming reactive $[Rh(\eta^2\text{-dieneH}_2)(L_2)SB_9H_{10}]^+$ intermediates that would finally result in the incorporation of the $\{Rh(L_2)\}$-fragment into the cluster (Scheme 3).

In the presence of PPh_3 and molecular hydrogen, similar routes involving either substitution or hydrogenation of the diolefins can be envisioned. Thus, gas chromatography of the reaction mixtures showed that for the cod-containing reactants there is formation of the alkene cyclooctene

whereas, for the nbd-reagents, we found free nbd and its reduction product, norbornane, $nbdH_4$. These results suggest that interplay of PPh_3/H_2(g) with the Rh(I) salts is most likely to yield intermediates of the type [Rh(η^2-diene)(L_2)(PPh_3)]$^+$ and [Rh(η^2-dieneH_2)(L_2)(PPh_3)]$^+$, which could react further with (i) H_2(g) and PPh_3 to give the Rh(III) complexes [Rh-$(H)_2(PPh_3)_2(L_2)$]$^+$ or with (ii) the thiaborane anion $[SB_9H_{12}]^-$ to afford the *nido*-rhodathiaboranes **13**−**15**. In the case of [Rh(η^4-nbd)(L_2)]$^+$, the reactions appear to proceed through two complementary pathways: (i) substitution of the diolefin norbornadiene; (ii) full reduction of the diene to norbornane. In contrast, [Rh(η^4-cod)(L_2)]$^+$ appears to react after partial reduction of the diolefin cyclooctadiene.

In view of these mechanistic suggestions, the differences in the observed reactivity of the cod−Rh salts versus the nbd−Rh analogues could be, in a first instance, the consequence of the relative labilities and hydrogenation rates of the Rh-bound diolefins. Thus, it is known that the cod ligand in [Rh(cod)$(PR_3)_2$]$^+$ complexes is hydrogenated at rates a hundred times slower than the nbd group in analogous Rh-(I) complexes,[28] and although the nbd−Rh bond is thermodynamically more stable than the cod−Rh linkage, nbd−Rh complexes are more labile with respect to diene exchange.[29] Therefore, if either partial substitution or hydrogenation of the diene is playing a role in the reactions between the Rh-(I) complexes and the $[SB_9H_{12}]^-$ thiaborane, the cod−Rh salts **1**, **3**, and **5** should feature longer reaction times than the nbd analogues **2**, **4**, and **6**. Moreover, the lower reaction rates of the Rh-coordinated cod ligand toward either substitution or hydrogenation could favor alternative reaction pathways that, as observed for the salts **1**, **3**, and **5**, may afford the new species that we propose to be *exo*-polyhedral rhodium complexes with the *arachno*-thiaborane $[SB_9H_{12}]^-$ (Scheme 3).

The observed enhancement of reactivity of the [Rh(η^4-diene)$(py)_2$]$^+$ complexes with the $[SB_9H_{12}]^-$ anion in **7** and **8** versus their [Rh(η^4-diene)(L_2)]$^+$ congeners (L_2 = bpy, Me_2bpy, phen) may be due to the higher lability and conformational flexibility of the pyridine ligands compared to the chelating N-heterocycles, which, consequently, may result in the formation of intermediates with lower activation energies toward {Rh$(py)_2$}-fragment insertion in the thiaborane cage. Interestingly, the reactivity of **7** and **8** depends markedly on the solvent, and thus, as described above, when dissolved in CH_2Cl_2, the salts immediately afford the rhodathiaborane **12** at room and at low temperatures. In contrast, **7** and **8** are surprisingly stable in CH_3CN, where they may be studied at room temperature without apparent decomposition for hours.

The dramatic decrease in the reactivity of the pyridine-containing salts **7** and **8** in acetonitrile can be rationalized as consequence of the interaction of the solvent with the square-planar 16-electron compounds [Rh(η^4-diene)$(py)_2$]$^+$ resulting in an effective protection of the rhodium complexes against reaction with the thiaborane anion $[SB_9H_{12}]^-$. Formation of 5-coordinate [Rh(η^4-diene)$(NCCH_3)(py)_2$]$^+$ adducts in fast equilibrium with 4-coordinate [Rh(η^4-diene)$(py)_2$]$^+$ complexes can be a dominant factor in shielding the rhodium complexes toward formation of reactive [Rh(η^2-diene)$(py)_2$-(SB_9H_{12})] species.

In contrast to the starting materials **1**−**8**, the dihydride rhodium(III)-containing salts **19**−**21** are stable in solution and the solid state. This behavior indicates that the dihydride complexes [Rh$(H)_2(L_2)(PPh_3)_2$]$^+$ do not react with the thiaborane anion $[SB_9H_{12}]^-$ to give 11-vertex {Rh$(L_2)(PPh_3)$} *nido*-rhodathiaboranes. Therefore, to obtain good yields of the rhodathiaboranes [8,8-(L_2)-8-(PPh_3)-*nido*-8,7-$RhSB_9H_{10}$] **13**−**15** from the treatment of the diene−Rh(I) salts **1**−**6** with PPh_3 in an H_2(g) atmosphere, the reactions of putative [Rh-(η^2-diene)$(L_2)(PPh_3)$]$^+$ or [Rh(η^2-dieneH_2)$(L_2)(PPh_3)$]$^+$ intermediates with the thiaborane anion to lead to insertion of the {Rh$(L_2)(PPh_3)$} moiety into the cluster framework should be faster than for the oxidative addition of H_2(g) and PPh_3 coordination to the rhodium center, which alternatively affords the corresponding rhodium(III) dihydrides. In the case of the [Rh(cod)(phen)]$^+$ cation, the rate of {Rh(PPh_3)(phen)}-fragment insertion into the thiaborane appears to be slower than for the formation of the Rh(III) complex with either excess or stoichiometric amounts of phosphine, yielding, therefore, exclusively the [Rh$(H)_2$(phen)$(PPh_3)_2$]$^+$ species. In contrast, the reactivity of the bpy and Me_2bpy counterparts [Rh(cod)(L_2)]$^+$ to give either the PPh_3-ligated rhodathiaboranes or the hydride complexes depends on the concentration of phosphine.

The 11-vertex rhodathiaboranes **9**−**12** are new examples of borane-based clusters containing square-planar 16-electron transition-element centers, which deviate from the classical Williams−Wade cluster-geometry electron-counting relationship.[22] According to this interpretation, the *nido*-structural architecture would formally require 13 skeletal electron pairs (sep). However, an electron count of the constituent vertices gives only 12 sep for the clusters. Thus, **9**−**12** are formally unsaturated, albeit with the unsaturation localized on the 16-electron rhodium center. In an alternative description, therefore, these rhodathiaboranes may be regarded as complexes of 16-electron {Rh(L_2)}$^+$ metal moieties with the [*nido*-SB_9H_{10}}$^-$ group acting as tetrahapto ligand with bidentate character: this implies a two-orbital metal-to-heteroborane bonding interaction and a corresponding basic four-orbital square-planar metal coordination sphere. This alternative view of the 11-vertex *nido*-clusters **9**−**12** as square-planar 16-electron complexes reveals the presence of a Lewis acidic site at the metal center, which rationalizes the observed reactivity of these compounds with Lewis bases.

Finally, it is noteworthy that compounds **9**−**12** decompose slowly over days in CH_2Cl_2 under an argon atmosphere to yield insoluble materials. This instability contrasts with the behavior of the phosphine-ligated analogues [8,8-$(PPh_3)_2$-*nido*-8,7-$RhSB_9H_{10}$] and [8,8-(dppe)-*nido*-8,7-$RhSB_9H_{10}$], which are stable for weeks in CH_2Cl_2 solution at room temperature. Interestingly, the PPh_3 and $NCCH_3$ adducts are also more stable than their corresponding [8,8-(L_2)-*nido*-8,7-

(28) Schrock, R. R.; Osborn, J. A. *J. Am. Chem. Soc.* **1976**, *98*, 2134−2143.
(29) Volger, H. C. M. M. P.; Gaasbeek, M.; Hogeveen, H.; Vrieze, K. *Inorg. Chim. Acta* **1969**, *3*, 145−150.

$RhSB_9H_{10}$] (L_2 = bpy, Me_2bpy, phen) precursors and, within the {$Rh(L_2)(L')$}-containing series **13**−**18**, those with the phosphine ligands exhibit higher stability than the $NCCH_3$ derivatives. This may be due in part to the dissociation of the Rh-coordinated acetonitrile ligand that has been observed to occur when the $NCCH_3$-coordinated *nido*-rhodathiaboranes are dissolved in CH_2Cl_2.

Conclusions

The reactivity of the new organometallic/thiaborane salts **1**−**8** is controlled by the square-planar rhodium(I) complexes. The nbd−Rh complexes drive the transformation of these salts toward insertion of the rhodium centers into the {SB_9H_{10}}-cluster framework. In contrast, the cod−Rh complexes promote alternative reaction pathways that in the case of the phen-containing salt **5** afford a new compound, which we propose as an *exo*-polyhedral rhodium complex of the thiaborane anion [6-*arachno*-SB_9H_{12}]. The square-planar nbd−Rh(I) reagents yield faster reactions and higher selectivities than their cod−Rh congeners. These results appear to be a consequence of the higher kinetic lability of the nbd ligand and its faster hydrogenation relative to the cod diene.

New convenient synthetic procedures toward metallathiaboranes that contain N-heterocyclic ligands have been developed. In view of their low stability relative to previously reported Rh−phosphine analogues, the new 11-vertex *nido*-species **9**−**12** can be regarded as "slightly stabilized" rhodathiaboranes, suggesting that other Lewis bases could generate clusters that incorporate {$Rh(L_2)(L')$} moieties (where L_2 = N-heterocyclic chelating ligand, L' = Lewis base). A comparative chemistry in the series of isoelectronic 11-vertex *nido*-rhodathiaboranes could, therefore, be developed.

Acknowledgment. This work was supported by the Ministerio de Educación y Ciencia (MEC, Spain) (Factoría de Cristalización, CONSOLIDER INGENIO-2010, and Grant 2003-05412). R.M. thanks the MEC-Universidad de Zaragoza for his Research Contract in the framework of the "Ramón y Cajal" Program.

Supporting Information Available: Details of the synthesis and isolation of (a) the salts **1**−**8**, (b) the rhodathiaboranes **13**−**15**, and (c) the CO−Rh salts **22**−**24**, NMR spectra of the transformation of **1**, **5**, and **7** in CD_2Cl_2 at different times, NMR spectra of the proposed *exo*-polyhedral rhodium complex that results from **5**, NMR spectra of compound **9** in $CDCl_3$ with addition of CH_3CN, X-ray diffraction details, atomic coordinates, bond lengths and angles, isotropic and anisotropic displacement parameters, and CIF files, and rate constants for PPh_3 exchange at different concentrations. This material is available free of charge via the Internet at http://pubs.acs.org.

IC700648Z